Carbon

Lightweight, Few-Layer Graphene Composites with Improved Electro-Thermal Properties as Efficient Heating Devices for De-Icing Applications

--Manuscript Draft--

Manuscript Number:	CARBON-D-21-02087R1
Article Type:	Research Paper
Keywords:	few-layer graphene sheets; expanded graphite exfoliation; conductive polymer-based composites; FLG/polymers manufacturing procedures; de-icing properties
Corresponding Author:	Giuliano Giambastiani, Ph.D. Institute of Chemistry of OrganoMetallic Compounds Florence, ITALY
First Author:	Giuliano Giambastiani, Ph.D.
Order of Authors:	Giuliano Giambastiani, Ph.D.
	Housseinou Ba
	Lai Truong-Phuoc
	Thierry Romero
	Christophe Sutter
	Jean-Mario Nhut
	Guy Schlatter
	Cuong Pham-Huu
Abstract:	Conductive polymer-based composites with electro-thermal properties are gaining great interest in several challenging technological applications. They are more and more employed as integrated heating devices within smart buildings or de-icing materials for application spanning from the aerospace sector to that of civil engineering. Their lightweight character along with high thermal efficiency and moderate production costs, make them highly attractive alternative to the use of classical electrothermal systems based on costly and heavier metals. Here we describe a convenient approach to the preparation of few-layer graphene-based (FLG) polymer composites obtained from the surface coating of selected polymer matrices with an electrically conductive and thin FLG “skin”. We demonstrated that low FLG concentrations at the outmost polymer surface, together with an excellent and homogeneous surface adhesion, allowed to get fast-responsive and lightweight heatable devices while keeping unchanged the properties of the underlying polymers. A controlled low-temperature post-treatment of the composites ensured an extremely high adhesion of FLG sheets to the hosting polymer matrix. The as-prepared composites have shown fast on/off heating response and exceptional performance once employed as lightweight and low-power heating devices with de-icing properties.

Lightweight, Few-Layer Graphene Composites with Improved Electro-Thermal Properties as Efficient Heating Devices for De-Icing Applications

Housseinou Ba,[a,b,] Lai Truong-Phuoc,[a] Thierry Romero,[a] Christophe Sutter,[a]*

Jean-Mario Nhut,[a] Guy Schlatter,[a] Giuliano Giambastiani,[a,c,] Cuong Pham-Huu [a,]**

[a] *Institute of Chemistry and Processes for Energy, Environment and Health (ICPEES), ECPM, UMR 7515 of the CNRS and University of Strasbourg, 25 rue Becquerel, 67087 Strasbourg Cedex 02, France. Email: giambastiani@unistra.fr and cuong.pham-huu@unistra.fr*

[b] *Present address: BlackLeaf SAS, 23, rue Ristelhuber, 67100 Strasbourg, France. Email: hba@blackleaf.fr*

[c] *Institute of Chemistry of OrganoMetallic Compounds, ICCOM-CNR and Consorzio INSTM, Via Madonna del Piano, 10, 50019 Sesto F.no, Florence, Italy. Email: giuliano.giambastiani@iccom.cnr.it*

Abstract

Conductive polymer-based composites with electro-thermal properties are gaining great interest in several challenging technological applications. They are more and more employed as integrated heating devices within smart buildings or de-icing materials for application spanning from the aerospace sector to that of civil engineering. Their lightweight character along with high thermal efficiency and moderate production costs, make them highly attractive alternative to the use of classical electrothermal systems based on costly and heavier metals. Here we describe a convenient approach to the preparation of few-layer graphene-based (FLG) polymer composites obtained from the surface coating of selected polymer matrices with an electrically conductive and thin FLG "skin". We demonstrated that low FLG concentrations at the outmost polymer surface, together with an excellent and homogeneous surface adhesion, allowed to get fast-responsive and lightweight heatable devices while keeping unchanged the properties of the underlying polymers. A

controlled low-temperature post-treatment of the composites ensured an extremely high adhesion of FLG sheets to the hosting polymer substrate. The as-prepared composites have shown fast on/off heating response and exceptional performance once employed as lightweight and low-power heating devices with de-icing properties.

Keywords: few-layer graphene sheets; expanded graphite exfoliation; conductive polymer-based composites; FLG/polymers manufacturing procedures; de-icing properties.

1. Introduction

Polymer-based composites featuring with thermo-electrical properties and their manufacturing techniques have triggered great interest within the scientific community during the last decades as many of them have found concrete applications in several daily-life devices.[1-3] While many organic polymers behave as poor electrical conductors or even act as electrical insulators, their conductivity can be improved through their blend with conductive fillers such as carbon fibers, carbon nanotubes (CNTs), graphene[4-8] as well as a wide variety of metal particles and/or nanowires.[9] Such an approach has been applied to the production of a series of lightweight polymer composites with improved electrical and thermal properties compared to their unfilled counterparts. Anyhow, the blend of a “hosting” polymer with a “guest” conductive filler (even for low concentrations of the latter) can deeply and detrimentally impact on the physical properties of the pristine polymeric network. Depending on the "host-guest" combination, important morphological and chemico-physical drawbacks can limit the widespread exploitation of these hybrid materials. Accordingly, large and costly efforts have been devoted to the optimization of manufacturing techniques including the rational use of coupling agents suitable to improve the fillers/polymer interfacial properties, optimize the electrical percolation threshold and prevent detrimental fillers segregation phenomena within the hosting polymeric networks.[10-12] The

current literature lists several exhaustive and comprehensive review articles dedicated to the synthesis and application of these lightweight polymer composites.[9, 13-15] Looking beyond their most traditional areas of application, conductive polymer-based composites can be employed as lightweight heating devices, integrated heating systems within smart buildings or de-icing materials for application spanning from the aerospace sector, to the civil engineering applied to the development of wind turbines operated under cold climate conditions and telecommunications devices.[16-20] Heatable polymer-based composites can also find application for the temperature control on submarine pipelines, hence replacing more costly metal-based technologies,[21] or they can even replace specific metal portions in aircrafts with significant weight reductions and subsequent energy consumption decrease.[22]

Finally, the formation of ice deposits on aircrafts or wind turbines blades can also cause serious structural, safety and aerodynamic issues. Indeed, they can overload the structures, alter their physical properties and in worse cases cause mechanical failure or loss of performance with subsequent serious efficiency and safety concerns.[16, 17, 23, 24] To face with these technical inconveniences linked to the ice or frost removal from icy surfaces, chemical deicers are commonly exploited that prevent the ice adhesion and make its removal easier.[25] However, their widespread use poses several technical, economic and environmental concerns linked to their relatively high costs, also associated to their on-site delivery and potential impact on the environment.

Rapid and low-energy demanding de-icing procedures based on the use of functional composites is therefore a highly desirable and more sustainable alternative to the costly and environmentally unsafe chemical de-icing procedures.[26] In a recent report, Karim *et al*. have described a scalable process of the manufacturing of graphene-coated glass rovings for the preparation of glass/epoxy composites with low-power and effective de-icing applications.[8] Despite the general process feasibility demonstrated by these authors, the use of glass rovings as supports for the thermo-electrical graphene phase and their integration into a vacuum-infused epoxy–glass fabric can pose technical concerns to the ultimate mechanical stability of the resulting

composite as well as its lightweight character. This aspect can become even more critical once referred to the composite downstream application. Indeed, the use of lightweight and electro-thermally heatable materials can largely and positively impact on the overall energy balance of a process or an application.

The search for alternative procedures to the preparation of heatable polymer-based composites as lightweight materials that retains the mechanical properties of the hosting polymer matrices almost unchanged, is a challenging research area where room is still available for important technological improvements. There are no doubts that the production of heat-responsive polymer-based composites obtained from the use of low-concentrations of conductive fillers, with a very low extra-weight increase and without altering the inherent physical and mechanical properties of the host polymer network, is a highly desirable target in material science. On this regard, we feel that the effective and stable surface coating of different polymer networks using an easily scalable protocol for the preparation of FLG-based paints can represents an appropriate answer to the production of low-power heatable devices to be engaged as lightweight materials with de-icing properties. On a similar ground, recent achievements in the field of the graphene scalable production, have successfully demonstrated its use in the form of low-electrical resistance inks for the large-area printing of flexible electronics.[27, 28]

Whatever the final application, the choice of graphene as the electrically conductive allotropic form of a carbon phase is generally dictated by its unique chemico-physical properties such as its high surface area,[29] and mechanical strength[30] together with its superior thermal conductivity (≈ 5000 W/mK)[31] compared to other forms of carbon [*i.e.* CNT (≈3000 W/mK) and amorphous carbon (≈1 W/mK)].[32] In addition, its high aspect-ratio[33] makes possible to form percolative electric networks already at very small amounts of C-loading with important benefits on the ultimate weight of the composite.

In this work we describe a coating procedure for the preparation of low-power heatable polymer-based composites, obtained from their surface "painting" with an electrically conductive "skins" made of FLG sheets.

2. Experimental Section

2.1 Materials and methods

Commercial polymers with various composition have been selected as hosting networks for the preparation of conductive composites. Flexible Polyurethane foam sheets [PU at variable PPI (*pores-per-inch*)] were purchased from Azur-caoutchouc France (www.azur-caoutchouc.com/index.cfm) and cut out with the shape of hollow cylinder an electro-thermal heating wire cutting tool, acrylonitrile-butadiene-styrene (ABS) fusion ultrafuse BASF wire for 3D-printing (product n° BSF921558 white), d = 1.06 g cm^{-3}; $T_g \approx 105$ °C was obtained from Filimprimante3D (www.filimprimante3d.fr), poly-methyl-methacrylate [PMMA plates – 2cm x 2cm x 5mm(h) or 9cm x 5cm x 3mm(h) were acquired from Plaque plastique France (https://plaqueplastique.fr/), d = 1.18 g cm^{-3}, $T_g \approx 105$ °C], and poly-etheretherketone (PEEK) was kindly provided by Stelia Aerospace, www.stelia-aerospace.com in the shape of 15 cm x 5 cm x 0.6 cm plates and pipes $\varnothing_{ED}$ = 2.55 cm; $\varnothing_{ID}$ = 2.35 cm; d = 1.27 g cm^{-3}). Unless otherwise stated, all commercial polymers and 3D-printed polymer supports used in the manuscript were thoroughly washed with pure water and dried at room temperature to remove all surface contaminants and dust traces before undergoing the coating/drying treatment. The high temperature silicone resin used for the white painting of FLG deposits in polymer-based composites was purchased from MOTIP DUPLI B.V. (https://www.motip.com). The 3D printer used for preparing the ABS aircraft model is the 3D 3D FreeSculpt "EX1-Basic" equipped with the 3D software INVENTOR (Professional-grade 3D CAD software for product design and engineering). Power generators used for testing the electro-thermal properties of the FLG-polymer-based composites are: ELC DC power supply AL

936 N (for low voltage supply, up to 30 V, max 5A) and EA Elektro-Automatik DC supply EA-PS 9360-40 3U (0 → 360V, 40A). Electrical conductivity (σ = s m^{-1}) was measured using a four-points probe Potentiostat Bio-Logic SP300 (Grenoble, France) while the sheet resistance (R_S = Ω/□) was determined with a four-points probe Mitsubishi Chemical Analytech Loresta-GX (MCP-T700). The temperature value at the surface of each composite was determined (unless otherwise stated) by a K type Ø 0.5 mm thermocouple attached directly to the graphene surface and connected to an external device equipped with a PID (Proportional Integral Derivative) controller. The collected data were recorded and elaborated by a dedicated software coded under LabVIEW (https://www.ni.com/it-it/shop/labview.html) that allowed to monitor the temperature evolution *vs.* time.

2.2 Preparation of FLG aqueous suspensions at variable concentrations and airbrush-painting or dip-coating procedure for the preparation of conductive polymer-based composites.

Few-layer graphene (FLG) suspensions were prepared through a tip sonication of an aqueous expanded graphite (EG) suspension in the presence of a hydrocolloid (Karaya gum) as exfoliating and stabilizing agent, according to our proprietary procedure.[34, 35] More synthetic details on the synthesis of FLG suspensions at variable concentrations (between 3 g/L and 10 g/L) are provided elsewhere.[28, 36] In a typical exfoliation procedure, 5 g of expanded graphite (EG) and 0.5 g of karaya gum, were added to 1L of distilled water. The exfoliation was carried out in a BRANSON digital sonifier (SFX550 Model made by EMERSON Co. with a nominal power of 400 W at 20 kHz, equipped with a 1/2" disruptor horn) operating at 40 W power (10 % of the nominal power) at *r.t.* for 2 h. Throughout the sonication process, the mixture was stirred (300 rpm) by a magnetic stir bar while keeping constant its temperature at 35 ± 5 °C by means of an external water-filled cooling jacket. Afterwards, the FLG suspension was used as such without any further purification/filtration treatment. The coating process was performed using an airbrush-painting mode (***CAUTION!***

airbrush-painting with FLG suspensions have to be rigorously handled in a well ventilated laboratory fume hood)[35] or a classical dip-coating procedure. As for the latter procedure, a selected 3D polymer network was soaked in the graphene coating bath at room temperature (19-21°C) and maintained there for few seconds (15-40 sec. whatever the *pores-per-inch* of the selected polymer) before being removed, gently fluxed with a stream of compressed air, left to drain on a filter paper and oven dried. Whatever the coating/painting procedure used, each polymer underwent an oven drying step at a given temperature selected on the basis of the glass transition (T_g) or melting temperature (T_f) of the hosting polymer matrix after each airbrush-painting or dip-coating treatment. The drying phase was accomplished in a pre-heated oven set at the temperature of 60 ± 5 °C, 140 ± 5 °C or 160 ± 5 °C for PU foams, PEEK pipe/plate or PMMA bricks, respectively. The deposition/drying process was repeated till the polymer surface was covered with a homogeneous FLG layer whose surface resistance (sheet resistance, R_S = Ω/□)[37] or electrical conductivity (σ = S m^{-1}) were measured by a four-points probe system. For all samples prepared by airbrush-painting technique we statistically assumed a roughly 20% of the irrorated FLG suspension lost during the treatment. Such a percentage was roughly determined on the basis of the weight increase measured for a series of polymer-based composites prepared by airbrush painting method and using FLG suspensions at variable concentration (comprise between 3 and 10 g/L of FLG). Accordingly, a series of blank experiments using different hosting polymers and FLG suspensions have been carried out to estimate the average % of FLG lost throughout the airbrush painting process.

2.3 Characterization techniques

Scanning electron microscopy (SEM) was carried out on a Zeiss 2600F with a resolution of 5 nm. The sample was deposited onto a double face graphite tape to avoid charging effect during the analysis. *Transmission Electron Microscopy* (TEM) was carried out on a JEOL 2100F working at 200 kV accelerated voltage, equipped with a probe corrector for spherical aberrations and a point-to-point resolution of 0.2 nm. For samples analysis preparation, an ethanol suspension of FLG was

ultrasonicated for 5 minutes as to get a homogeneous and not-settling down suspension that was evaporatively casted on a copper grid covered with a holey carbon membrane for observation. *Thermogravimetric analysis* (TGA/DTG) was performed on a *thermo-gravimetric* (TG) analyser (Thermo) using a temperature program comprise between 30 and 900 °C at a heating rate of 10 °C/min, under air with a stream of 60 mL/min. *X-ray photoelectron spectroscopy* (XPS) was carried out in an ultrahigh vacuum (UHV) spectrometer equipped with a VSW Class WA hemispherical electron analyser, using a monochromated Al Kα X-ray source (1486.6 eV) as incident radiation. Survey and high-resolution core region spectra were recorded in constant pass energy mode (90 and 44 eV, respectively). The CASA XPS program with a Gaussian-Lorentzian mix function and Shirley background subtraction was employed to deconvolute the XP spectra. *Raman* spectra were recorded on a LabRAM ARAMIS Horiba Raman spectrometer equipment. Spectra were acquired in the 500 - 4000 cm^{-1} range at the laser excitation wavelength of 532 nm. For this spectroscopy, the sample was deposited on a glass substrate by spin-coating, and it was properly dried before any measurement.

3. Results and Discussion

Representative TEM micrographs of FLG sheets as prepared with our proprietary protocol applied to a 5g/L suspension of expanded graphite (EG - see experimental section for details) are presented in Figs. 1A-D. Images show 2D graphene flakes of several micrometers of lateral size. HRTEM images (Figs. 1C-D and Fig. S1) recorded on the sample show that graphene flakes were formed by few (4-8) and well-defined stacked layers. These evidences well corroborate with Raman spectroscopy (Fig. 1E) whose more prominent components (D, G and 2D at ≈ 1340 cm^{-1}, ≈ 1580 cm^{-1} and ≈ 2660 cm^{-1}, respectively),[38] peaks shape, their full width at half maximum (FWHM) and Raman shift values were consistent with those reported for a few layer graphene sample.[39, 40] Similarly, the TGA profile recorded for the powdery sample in the 40 to 900 °C temperature

range (heating rate: 10 °C/min, under air 60 mL/min. - Fig. S2B) indicated the high resistance of FLG sheets to their oxidation (occurring quantitatively within 650 and 730 °C) whose temperature value ($\%_{max}$ weight loss - DTG) well-matched with the value fixed for the TGA-based quality control for bulk FLG powders.[40] These spectroscopic, gravimetric and morphological features were in line with the at the beginning of Therefore, all these data were consistent with the high efficiency of the adopted top-down protocol to produce FLG sheets instead of graphite flakes.

The XPS survey spectrum of FLG sheets (Fig. S2B) showed only a relatively small amount of oxygen with respect to a prominent carbon peak, while no other elements were detected in the sample. The deconvoluted high-resolution XPS C 1s profile (Fig. 1F) accounts for the presence of several carbon species, with the Csp^2 and Csp^3 components at 284.6 and 285.1 eV, respectively, being largely predominant.[44] Minor components and little shoulders at higher binding energies (BEs) refer to variably oxidized carbon functionalities such as C-O (285.8eV), C–OH (286.6 eV) and C=O (288.2eV).[45, 46]

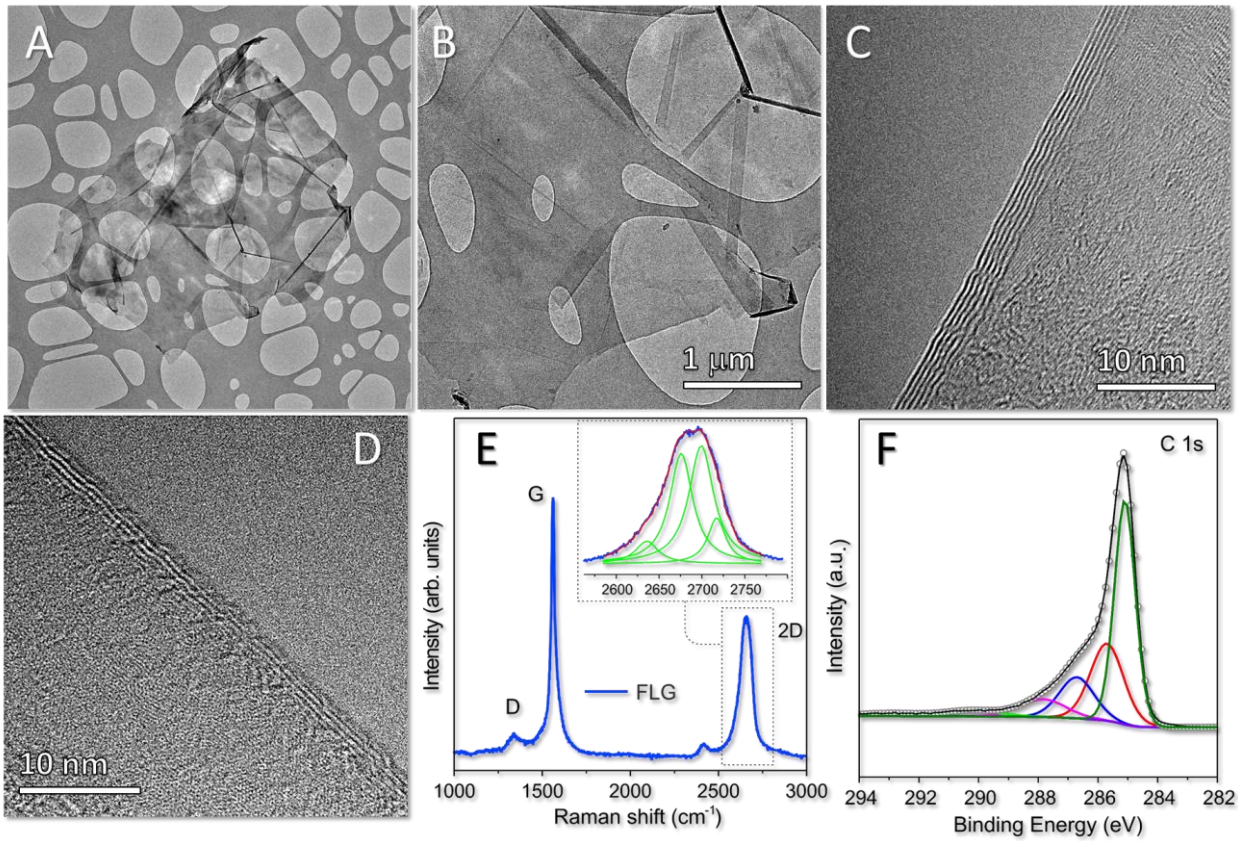

Fig. 1. A-B) HRTEM analysis of FLG sheets prepared from the dip-sonication of a 5g/L suspension of expanded graphite, using our proprietary exfoliation protocol. C) Raman spectrum of FLG micro-flake powders for 532 nm excitation. Inset refers to the 2D band deconvolution with Lorentzian curve fittings and accounts for a sample with a sheet-like morphology, typical of FLG.[47] C) HR XPS analysis of the C 1s core region of the FLG micro-flake sample.

With this mature exfoliation technology available for the easy and scalable production of aqueous suspensions of FLG sheets at variable concentrations, we started to investigate the preparation of a variety of conductive polymer-based composites throughout a polymer surface coating with a thin and conductive graphene layer. Depending on the nature and properties of the selected commercial polymer, the surface FLG deposit was accomplished by either airbrush painting or dip-coating modes. Whatever the nature of the applied coating procedure and the composition of the hosting polymer network, we succeeded in the preparation of robust composites with a thickness of the FLG coating from few microns to tens of microns depending on the applied coating method and the number of coating/drying cycles the composites underwent.

The following sections account for the synthesis, characterizing and application of a series of conductive polymer-based composites prepared with our technology as low-power electro-thermally heatable materials for the control and maintenance of their surface temperature or de-icing applications.

3.1 Synthesis of FLG-coated polymer composites (FLG/polymer) and their characterization

In a first trial, poly-methyl-methacrylate bricks [PMMA – 2 cm x 2 cm x 0.5 cm (h)] were airbrush-painted using benchmark water-based suspensions of FLG sheets prepared from either 1g/L or 3 g/L of EG. The bricks were maintained in an oven at 160 ± 5 °C till dryness (≈ 20 min) before being cooled down to ambient temperature and resubmitted to a second FLG airbrush-painting deposition. The whole procedure was repeated till the desired thickness of graphene (or graphene loading; wt.% - see Table 1) or electrical conductivity (σ) of the composite(s) were

reached (*vide infra*). Table 1 lists all main details of the operative procedure adopted for the preparation of nine FLG/PMMA composites along with the respective FLG contents and composite conductivity values. The oven-drying phase was intended to play a dual role in the composites preparation: 1) it was required to evaporate the excess of water deposited during the airbrush painting and 2) it was supposed to facilitate the FLG flakes adhesion to the polymer surface by releasing the mobility of macromolecular chains when it was heated just above its glass transition temperature (T_g). Such a transition does not alter the macroscopic properties of the composite but allows the establishment of a more intimate connection between the conductive FLG phase and the underlying polymer substrate. As Fig. 2A shows, the PMMA composite presents a highly homogeneous surface coating made of a layer-by-layer deposit of FLG sheets. SEM images (Fig. 2B-C) recorded at different magnifications highlight a smooth surface with the large graphene flakes reproducing the pristine roughness and surface imperfections at the hosting polymer matrix.

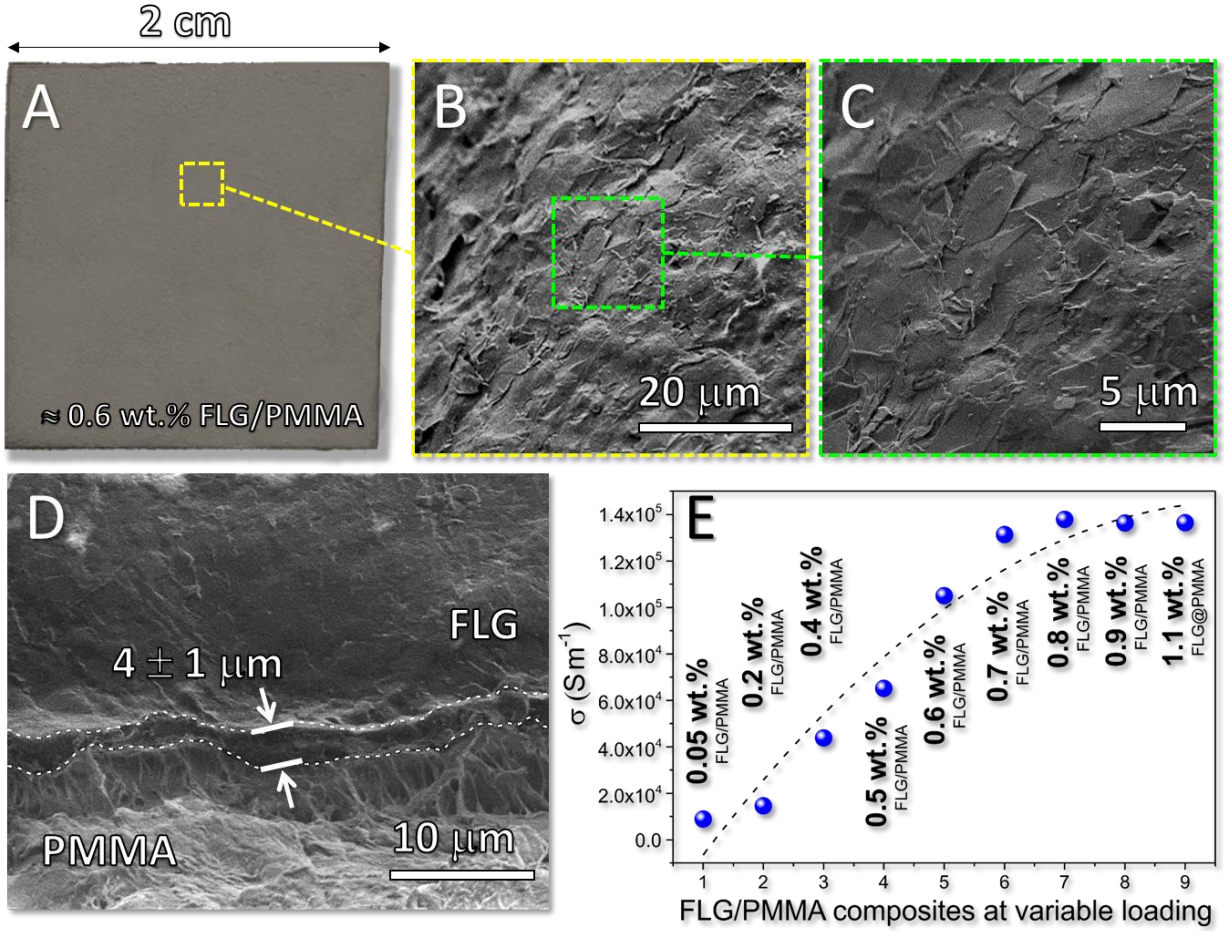

Fig. 2. A) Digital image of a PMMA brick airbrush-painted twice with an aqueous 3g/L FLG suspension (0.6 wt.% FLG/PMMA). B-C) SEM images at different magnifications of the composite surface. D) SEM image of a cross-section view of the aforementioned composite.[48] E) Electrical conductivity trend (s m^{-1}) measured by a four-points probe on each FLG/PMMA sample prepared at variable FLG loading (see Table 1 for details).

A cross-section view (Fig. 2D and Fig. S3) of the composite has allowed to estimate the thickness of the graphene deposit in a model composite prepared after two successive airbrush painting and drying cycles (Table 1, entry 5). The latter SEM picture illustrates the thickness of the graphene deposit and its intimate connection with the underlying amorphous phase of the polymer support. Noteworthy, FLG coating delaminates very rapidly if no thermal treatment is carried out. However, it can be inferred that the thermal treatment of the composite allows to establish a perfect interface adhesion and complete connectivity of the conductive graphene layer (4 ± 1 μm of thickness) with the roughness of the hosting polymer surface.

Table 1. FLG leading charged on each PMMA brick throughout successive airbrush-painting/drying cycles to prepare (0.05-1.1) wt.% FLG/PMMA composites.[a]

entry	$[FLG]_{conc.}$ (g/L) [b]	Cycles (n°) [c]	FLG used (mL) [d]	FLG deposit (mg/cm^2) [e]	FLG/PMMA (wt.%) [e]	Cond.(10^{-4}) ($S\ m^{-1}$) [f]
1	1	1	1.5	≈ 0.30	≈ 0.05	0.89
2	1	2	3	≈ 1.20	≈ 0.2	1.46
3	3	2	2	≈ 2.40	≈ 0.4	4.38
4	3	2	2.5	≈ 3.00	≈ 0.5	6.51
5	3	2	3	≈ 3.60	≈ 0.6	10.50
6	3	2	3.5	≈ 4.20	≈ 0.7	13.14
7	3	2	4	≈ 4.80	≈ 0.8	13.78
8	3	2	4.5	≈ 5.40	≈ 0.9	13.63
9	3	2	5.5	≈ 6.60	≈ 1.1	13.64

[a] Each airbrush-painting step was followed by a thermal treatment of the composite for 20 min in an oven set-up at 160 ± 5 °C before proceeding with the successive FLG deposit. [b] concentration of the FLG aqueous suspensions prepared with our exfoliation protocol. [c] n° of airbrush-painting/drying cycles applied to the composite preparation. [d] mL of the selected FLG suspension used for each airbrush-painting cycle. [e] calculated assuming a loss of the FLG suspension during the airbrush painting roughly estimated in 20% of the irrorated FLG paint. [f] Conductivity values measured by a four-points probe.

The FLG/PMMA composites prepared after successive airbrush painting/drying steps exhibited variable electrical conductivity. As Fig. 2E shows, the surface conductivity of the samples measured

by a four-points probe potentiostat, increased with the loading of the graphene deposit (coating/drying cycles). We measured an increase of σ value (s m^{-1}) from ≈ 1.0 10^4 S m^{-1} for the sample prepared at the lower graphene loading (a single deposition cycle – Table 1, entry 1), up to 1.3 10^5 S m^{-1} for the composite containing the 0.8 wt.% graphene loading (Table 1, entry 7). The high aspect ratio of FLG sheets allowed a small amount of the conductive deposit to form continuous percolation networks whose electrical conductivity steadily increased with the first coating cycles until reaching a plateau value.[6, 8, 49] However, FLG overloads (Table 1, entries 6-9) did not show any significant deviation in the samples' electrical conductivity whose values did not change appreciably (Fig. 2E and Table 1). It can be inferred that similar conductivity values will apply for different polymer-based composites prepared through the same airbrush-painting/drying procedure but realized starting from different polymer networks (*vide infra*).

It is evident that the electrical conductivity of the as-prepared samples was markedly higher - even at low FLG loadings - than that measured for conducting composites prepared through the more classical blending mode. In a recent contribution, Tour and co-workers reported on the preparation of a conductive composite using graphene nanoribbon (GNR) stacks blended in an epoxy resin as a Joule-heated structure for de-icing applications.[6] They claimed an electrical conductivity for their sample higher than 100 S m^{-1} for a GNR loading of 5 wt.%. Such a loading of the conductive filler was 10 times higher than the FLG content in our model 0.5 wt.% FLG/PMMA composite, with the blended GNR-composite exhibiting an electrical conductivity ≈ 650 times lower than ours (see Fig. 2E for the composite at 0.5 wt.% loading of FLG and Table 1, entry 4). Other less recent contributions have described the properties of polymer-based [*e.g.* polycarbonate (PC), polystyrene (PS) or polymethylmethacrylate (PMMA)] composites obtained by the filler suspension (*e.g.* carbon nanotubes) in an organic solution of a dissolved polymer followed by evaporative drop-casting and spin-coating to afford conductive polymer-based composites with even lower electrical performance in the face of markedly higher filler loadings.[50] Later, seminal review articles have systematically analyzed the electrical percolation[51] and the conductive

properties of a number of nanocarbon polymer-based composites as a function of the nature and production method of the C-nanofiller (CNT[52] or graphene[53]), its ultimate loading, the type of polymeric matrix and the polymer processing method. Whatever the parameters used in the composite synthesis, the σ/(filler wt.%) ratio can be even orders of magnitude lower that that measured on our FLG/polymer composites.

Although the higher σ value showed by our samples is obviously due to the conceptually different approach to the employment of the conductive filler (surface polymer coating *vs*. polymer/filler blend), the excellent adhesion strength of the conductive FLG layer obtained with different polymer networks, have strengthened our expectations for a successful application of these conductive composites prepared at low fillers loading within specific technological fields (*vide infra*). Moreover, the cheaper and simplest coating technology compared to that based on the formulation and elaboration of filler/polymer blends, allows to maintain the mechanical polymer properties while reducing to a large extent all technical limitations, physical and mechanical concerns and more challenging manufacturing procedures associated to the homogeneous dispersion of the conductive fillers in the polymer bulk.

Flexible polyurethane (PU) foams at variable *pores-per-inch* (8-50 ppi; Fig. S4) were shaped in the form of hollow cylinders before being employed as polymer networks for the coating/drying procedure with FLG suspensions. With this type of macroporous networks we experienced a coating methodology alternative to that of the airbrush painting. The coating step was performed by soaking PUs in the aqueous FLG suspension (prepared from a 10 g/L suspension of EG) before proceeding with the drying phase (60 ± 5 °C for 20 min). Two-three successive soaking/drying cycles were repeated till ≈ 1 wt.% FLG/PU composites are obtained. The higher the ppi value of the PU matrix, the higher the FLG content retained at the polymer surface after each soaking/drying cycle. Fig. 3 displays digital photos (A-B) and SEM images (C-D) recorded at variable

magnification on a representative 8 ppi PU foam (Fig. 3A, left) after 3 successive impregnation/drying cycles (Fig. 3A, right and 3B) as described above.

SEM images (Fig. 3C-D) revealed again a smooth surface coating of the PU matrix, made of a layer-by-layer deposit of graphene flakes. The most distinctive spectroscopic feature of the as-prepared composite was recorded at the XPS C *1*s core region (Fig. S5A vs. S5B), where an appreciable increase of the component at ≈ 285 eV was attributed to due to C-N bonds of the underlying PU network.[54]

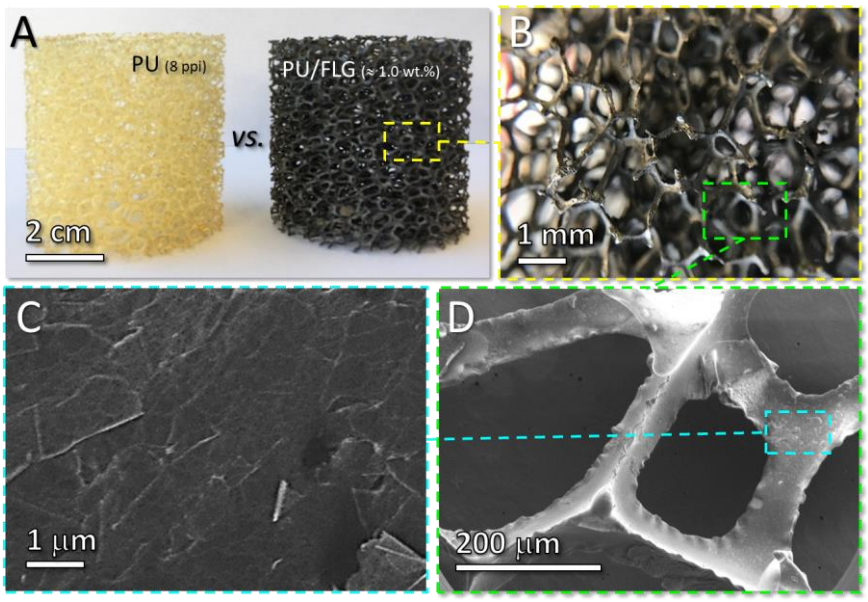

Fig. 3. A-B) Digital photos of a representative PU and PU/FLG composite. C-D) SEM images of PU/FLG at different magnifications showing the homogeneous FLG coating layer at the surface of the composite.

As a stability test for these light and hierarchically structured composites (≈ 1.0 wt.% FLG/PU) a dynamic measurement of their inherent resistance (Ω) as a function of the materials compression along their Z-axis was assessed. As expected for these flexible and mechanically compressible foam networks, the higher the material compression, the larger the extent of contact between the conductive FLG-coated PU fibers and the lower the materials electrical resistance. To this aim, the two opposite surfaces of each composite were put in contact with two copper electrodes and the materials were compressed stepwise along their Z-axis by means of a screwable plastic compressor

regulated at fixed distances (Fig. S6). Accordingly, the higher the % of foam compression, the lower the electrical resistance measured for the composites (Fig. 4A-B; from 2.8-4.1 kΩ down to ≈ 60-280 Ω for 8 ppi PU/FLG and 40 ppi PU/FLG composites, respectively). The release of the materials compression restored their pristine electrical resistance.

An additional stress test conducted on the model 30 ppi, ≈ 1 wt.% FLG/PU sample, confirmed the complete retention of the sample electrical resistance even after a sequence of 10 successive compression/decompression cycles (Fig. 4C). This last test was a further evidence of the high stability of the conductive surface coating prepared by the proposed dip-coating/drying protocol along with the full retainment of the mechanical properties of the hosting polymer matrix.

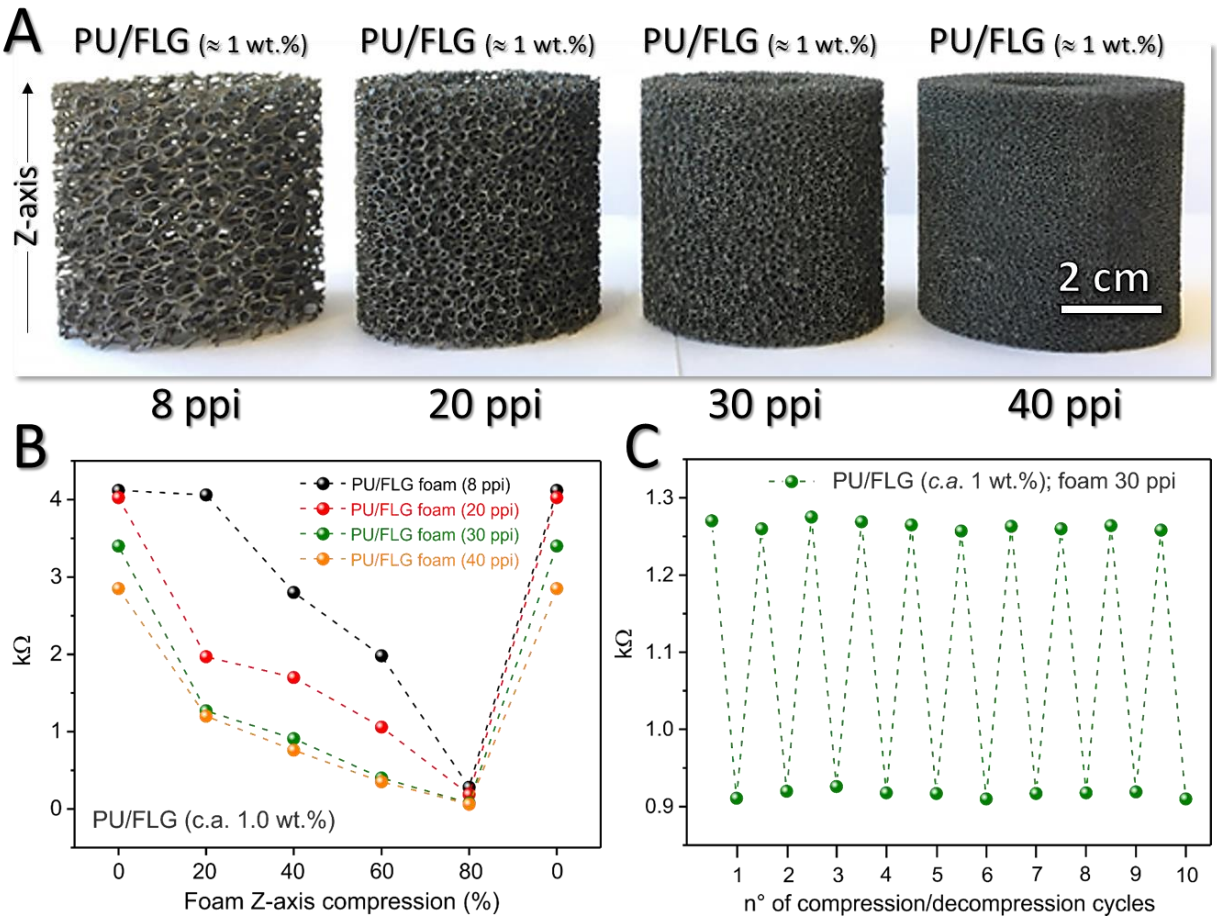

Fig. 4. A) Digital photos of ≈ 1 wt.% FLG/PU composites prepared by dip-impregnation/drying coating starting from commercial PU samples at variable ppi. B) Stress-compression test for the measurement of the material resistance as a function of the samples' compression degree. The latter is expressed as the % of foam deformation along its Z-axis [(5 cm - interfacial distance(cm))/50*100]. C) Dynamic measurement of the resistance (Ω) on the PU/FLG composite obtained from the 30 ppi foam under a sequence of 10 successive compression/decompression

cycles in the 40-60 % foam compression range. Each compression was maintained for 30 seconds before releasing the sample and allow it to reach its original shape.

The uniform and stable coating of a series of commercial polymers with a thin conductive FLG deposit, the easily scalable manufacturing process towards electrically conductive composites together with the retention of the pristine properties of the selected hosting polymer networks, have prompted us to investigate the potentialities of our coating technology for the preparation of low-voltage heating devices or electro-thermal materials for de-icing applications.

3.2 FLG/polymer composites as low-voltage heating devices or materials for electro-thermal de-icing applications

The preparation of uniformly coated polymers with a thin and stable conducting graphene layer is a highly desirable target to be reached for the development of composites to be exploited in electro-thermal applications. To properly represent this claim with concrete examples we started with a flat PMMA plate of 9 x 15 cm with a thickness of 3 mm. The thermoplastic polymer underwent two successive airbrush painting/drying cycles using 5 mL of a 6 g/L aqueous suspension of FLG sheets for each painting/coating cycle.

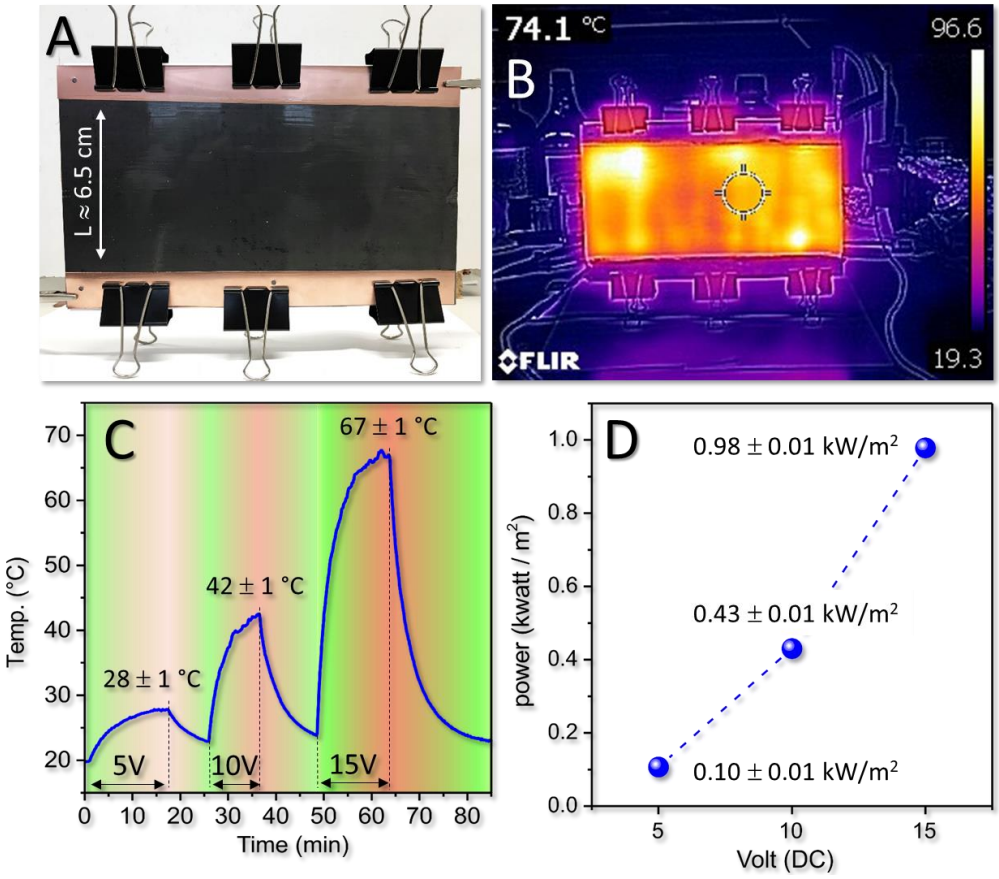

Fig. 5. A) Digital photo of the ≈ 0.1 wt.% FLG/PMMA composite in the setup used for the connection with the external power supply. B) Infrared thermal map of the temperature surface of the composite when an external low-voltage supply (15 V) was applied. C) Thermal mapping *vs.* time recorded by a K type ∅ 0.5 mm thermocouple located at the FLG surface. D) Thermal power density of the composite (kW/m^2) at different power supply values. Power was calculated as follows: P(W) = U(V) x I(A).

As a result, a ≈ 0.1 wt.% FLG/PMMA composite was obtained (≈ 0.35 mg/cm^2 of FLG; overall ≈ 48 mg of FLG) with a measured sheet resistance of 31.1 Ω/□. The conductive plate was then clamped between two copper electrodes (Fig. 5A, a length L of ≈ 6.5 cm was thus exposed to heating) and an external voltage of 5, 10 or 15 V was applied using a DC power generator.

The surface temperature of the composite was initially analyzed by a Forward Looking Infrared thermal camera (FLIR camera – Fig. 5B) and mapped at constant times (every 5 seconds) with a K type ∅ 0.5 mm thermocouple attached directly to the graphene surface and connected to an external controller equipped with a dedicated software for the temperature measurement. As Fig. 5C shows, the higher the applied potential (U), the higher the increase of the temperature at the surface of the

composite, with a limit value measured for the 0.10 wt.% FLG/PPMA of 67 ± 1 °C at an applied potential *U* of 15 V. Assuming that the temperature *T* of the FLG coating is homogeneous, the difference between its steady-state value T_{eq} and the ambient temperature (T_{air}) is given by the energy balance between heating by Joule effect and heat dissipation toward air on the top surface and the substrate at the FLG-polymer interface (see Fig.S7 for more details):

$$T_{eq} - T_{air} = \frac{U^2}{R_s h L^2} \qquad (1)$$

Where *L* is the length of the polymer plate and *h* a convection coefficient taking into account the overall heat dissipation. Here, we don't discuss the modelisation of the time evolution of the temperature which depends on the substrate thickness and its thermal properties (heat capacity and thermal conductivity). However, experimentally, the switch-ON/switch-OFF sequence shows that the coated surface of all samples were heated up to the target temperature value and cooled down to *r.t.* quite rapidly. This is explained by the thinness of the FLG coating that reduces any thermal inertia and moreover by the fact that the heat dissipation is mainly due to convection between the ambient air and the top surface of FLG, the FLG-polymer interface mainly behaving as an adiabatic surface. Compared to classical filler/polymer blended composites, such FLG coating allows a much more efficient heating of the outmost composite surface. Therefore, a low-FLG loaded (0.1 wt.%) composite with neither any appreciable increase of the polymer weight nor any alteration of its mechanical properties was homogeneously heated up to relatively high temperatures using a low-voltage power supply and was - in turn - rapidly cooled-down under open circuit conditions. Fig. 5D finally shows the thermal power density of the composite (kW/m^2) required to reach its target temperature value in the given time (see also Fig. 5C), and in function of the applied external potential (V). It should be stressed that with this technology, 1 m^2 of a 0.1 wt.% PMMA/FLG composite attached to an external DC power supply of 15 V is supposed to act as a planar and homogeneous thermal radiator absorbing roughly 1 kW to heat its surface up to 70 °C. This result

leaves us to imagine how such a technology can effectively contribute to produce indoor heating devices on a large scale in the place of more traditional electrical heaters or radiators. For the sake of completeness, we have also analyzed the heating response of the same 0.1 wt.% PMMA/FLG composite after covering its surface with a white acrylic paint (Fig. S8A). The latter, besides preventing the deterioration of the underneath graphene layers, can make easier and flexible the integration of such a heating device with its surroundings while keeping its heat radiation properties under the regime conditions almost unchanged (Fig. S8B).

As an additional example of conductive polymer-based composites for practical applications, we have evaluated our technology for the preparation of thermo-stabilized piping for the transport of thermo-sensitive fluids that can aggregate or undergo liquid-solid transition phase upon cooling, hence causing serious slowing of the fluid stream or - even worse - leading to irreversible damages to the whole transportation system. The presence of heatable pipe coat at its outmost surface only, holds the double advantage of preventing the occurrence of the fluid freezing passing through the pipe while avoiding its direct contact with a hot surface. The generally moderate thermal conductivity of any plastic pipe largely facilitates this task. Accordingly, we selected a semicrystalline thermoplastic polymer (*i.e.* Polyether-ether-ketone, PEEK) featuring with excellent mechanical and chemical resistance properties that are generally retained even when it was heated-up to temperatures as high as 200 °C. A first attempt was conducted on a short PEEK pipe of 6 cm in length, with an external diameter ($\varnothing_{ED}$) of 2.55 cm (wall thickness of 2 mm) and a lateral surface area of about ≈ 48.1 cm^2 (Fig. 6A). The pipe was airbrush-painted twice using the same procedure described above (see experimental section for details dealing with the drying step) with 3 mL of a 6 g/L aqueous suspension of FLG sheets for each painting/coating cycle (≈ 0.6 mg/cm^2 of FLG; overall ≈ 29 mg of FLG). Accordingly, a ≈ 0.5 wt.% FLG/PEEK composite with a sheet resistance (R_S) of 4.7 Ω/□ was prepared and electrically connected to an external DC power supply. With such a FLG loading (twice respect to that of the ≈ 0.1 wt.% FLG/PMMA plate), an applied external

voltage of 14 V (Fig. 6 and S9) was enough to rapidly increase the sample surface temperature up to 180 °C. A stepwise external low-voltage increase, showed that the pipe surface temperature could be varied gradually within a relatively wide range of values (Fig. S9). This aspect strengthened the high versatility of the composite as electro-thermal anti-/de-icing system where a fine control of the temperature was required as a function of the sample downstream application. The same technology was extended further to a longer PEEK pipe (1 m) that underwent an airbrush-painting/drying sequence of four successive cycles, each using 6 mL of a 6 g/L suspension of FLG. The as-obtained composite (≈ 0.14 wt.% of FLG) had an estimated overall graphene loading of ≈ 115 mg (≈ 0.14 mg/cm^2).

The graphene pipe coating was additionally covered with a heat-resistant silicone resin paint to prevent any mechanical damage of the thin conductive layer, leaving the pipe ends uncoated for the electrical connection to the external DC power supply. As Fig. 6C-D and Fig. S10 show, a supply of 40 V (DC) allowed the pipe to be gradually and homogeneously heated over 140 °C within a relatively short time (3 minutes). Noteworthy, the surface technology applied to the preparation of these polymer-based composites allowed to maintain the control of the temperature pipe even when partial damages of its surface would accidentally occur. As Fig. S11 shows, the pipe coating to its full outer surface ensures an extensive electrically conductive network that prevents the heating shutdown even in case of major structural damages.

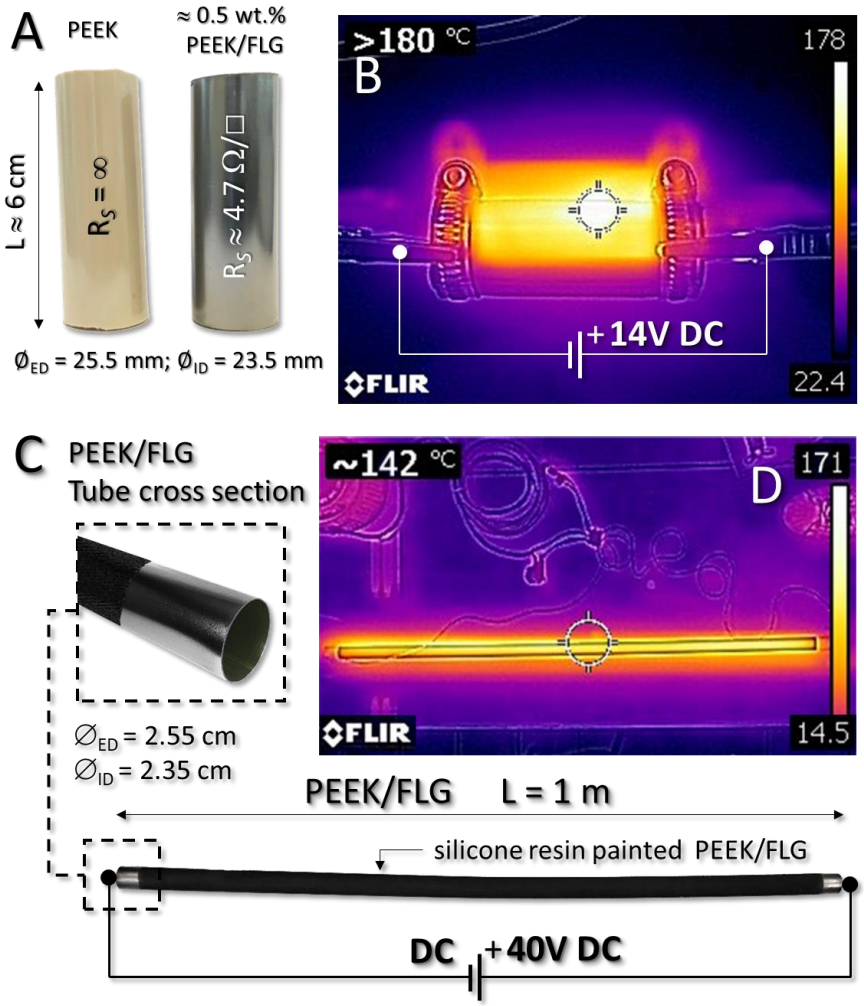

Fig. 6. A) Digital photos of two PEEK pipes before (left) and after the coating/drying (right) phase with a 6 g/L aqueous suspension of FLG sheets. B) Infrared thermal map of the composite surface when an external low-voltage supply (14 V) was applied. C) Digital photos of a 0.13 wt.% PEEK/FLG pipe (1 m) and its cross-section (inset) after the graphene-layer protection with a high-temperature resistant silicone resin black-paint. D) Infrared thermal map of the composite surface when an external 40 V (≈ 4.5 A) supply was applied.

The surface coating of a PEEK-pipe with a thin and electrically conductive graphene phase has prompted us to additionally investigate the use of alternative energy sources for the control of the electro-thermal properties of the composite. It is well known that magnetic nanoparticles (NPs) or simply electrically conductive networks, immersed in a magnetic field (H) produced by an alternating current (AC) generator, can act as target susceptors for the local conversion of the radiofrequency (RF) energy into heat [(induction heating (IH) or radiofrequency heating (RF)].[55] As far as conductive networks like graphene are concerned, the RF conversion into heat occurs

through the so-called Joule-heating effect due to the generation of eddy currents[56] (or Foucault currents) that concentrate heat to the outmost surface of the susceptor (Skin-depth effect).[57, 58] Accordingly, the PEEK/FLG pipe was housed within the coils of an induction heating setup equipped with a PID (Proportional Integral Derivative controller)-interfaced laser pyrometer directly shot over the graphene surface for a real-time control of the material temperature (Fig. 7A).

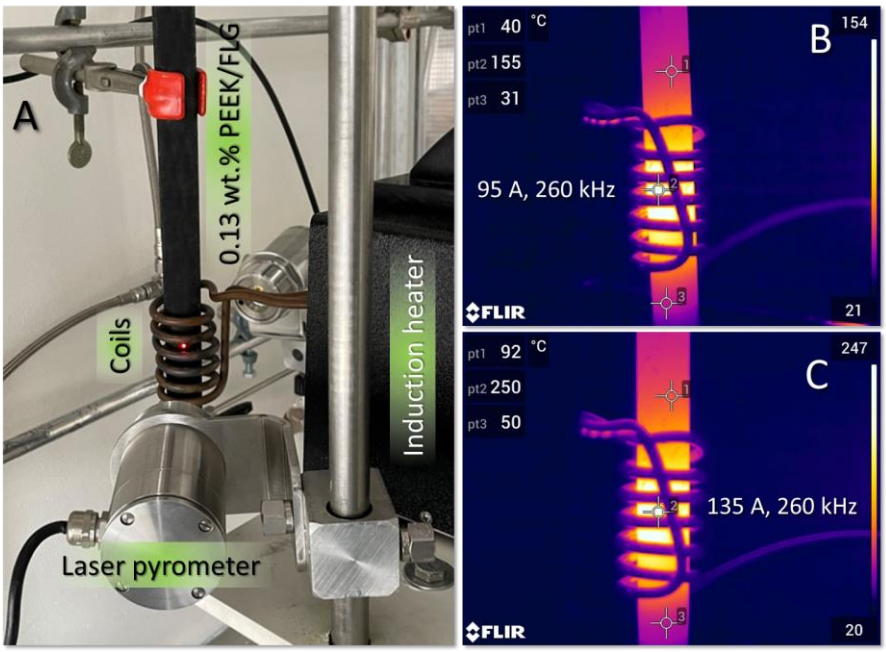

Fig. 7. A) Digital photo of the IH setup used for the 0.13 wt.% PEEK/FLG pipe heating. B-C) Infrared thermal maps of the composite surface under IH with two peak temperature values (pt2) of 155 and 250 °C for an applied current of 95 and 135 A (260 kHz), respectively. pt1 and pt2 refer to the pipe temperatures values measured outside the magnetic field (H) generated by the induction coils.

Afterwards, a variable current (I, 95 or 135A) at the constant frequency of 260 kHz was applied to the inductor coils as to generate the electromagnetic field (H). Such a RF-heating allowed a sudden increase of the composite surface temperature up to 155 °C (I = 95A) within 5 seconds that grew-up till 250 °C in less than 10 seconds for an applied current of 135 A. The system was then allowed to heat and cool down within a programmed temperature ramp in the 30-155 °C range and the thermal excursion was repeated on the pipe for more than 100 heating/cooling cycles without showing any appreciable alteration of its electro-thermal properties. Such a high thermal stability of the composite was ascribed to the excellent interface adhesion between the thin conductive graphene layer and the hosting PEEK network realized by the described coating protocol. In

addition, the graphene layer protection by a heat-resistant silicon paint allowed to prevent undesired graphene oxidations during the pipe heating, particularly when it reached high temperature values in a potentially oxidative environment.

The airbrush-painting/drying procedure was finally repeated on a 15 x 5 x 0.6 cm PEEK plate whose surface was deliberately coated with different graphene loadings. By this way we locally tuned the surface resistance of the FLG deposits (from 39 to 265 Ω/□) thus creating the conditions for a multi-thermal heating at the surface of the composite. As Fig. 8A shows, the PEEK surface was portioned into 5 sections and each of them was charged with a different graphene loading. The two external sections of the plate were covered with a relatively high loading of graphene as to optimize its electrical percolation and reducing the material surface resistance as much as possible. Afterwards these latter portions were clamped between two copper electrodes (Fig. 8A) and connected to an external power supply. The remaining (three) internal parts of the plate were charged with decreasing amounts of graphene (17, 10 and 4 mg) as to progressively increase their surface resistance (39, 97 and 265 Ω/□, respectively – Fig. 8A from left to right). Accordingly, the two peripheral regions (2.5 x 5 cm = 12.5 cm^2 each) were airbrush-painted with 2 x 5 mL of a 3 g/L FLG suspension as to get an average FLG loading of 1.9 mg/cm^2 (overall ≈ 24 mg on each portion). Then, 2 x 3.5 mL and 2 x 2 mL of the same FLG suspension were used to charge ≈ 17 and ≈ 10 mg of FLG on the third and second portion of the plate (≈ 1 mg/cm^2 and ≈ 0.6 mg/cm^2 for the 17.5 cm^2 and 15 cm^2 surfaces, respectively). Finally, the last (fourth) plate portion was airbrush-painted twice with 2 mL of a 1 g/L FLG suspension as to get roughly 0.2 mg/cm^2 of FLG (≈ 4 mg on 17.5 cm^2). The application of an external low-voltage (15 V) led to the rapid surface temperature rising at the composite. The thermal mapping recorded with the infrared thermal camera (FLIR camera – Fig. 8B) showed that an appropriate modulation of the graphene loading on different material portions was a convenient and elegant way to partitioning and regulate the temperature' surface of the composite as it was necessary based on its downstream application, while using a unique low-

voltage power input. A simple model (see Fig.S7 for more details) shows that the equilibrium temperature $T_{eq,i}$ of the area i is given by the following equation:

$$T_{eq,i} - T_{air} = \frac{R_{s,i}U^2}{h\left(\sum_i L_i R_{s,i}\right)^2} = kR_{s,i} \qquad (2)$$

Where $R_{s,i}$ is the sheet resistance of area i and L_i its length. Although the linear behavior between $T_{eq,i} - T_{air}$ and $R_{s,i}$ is not perfectly observed, probably due to more complex thermal exchange, expectedly, the higher the surface resistance of a given portion of the composite was, the higher its equilibrium temperature value (from 28.5 up to 57.2 °C).

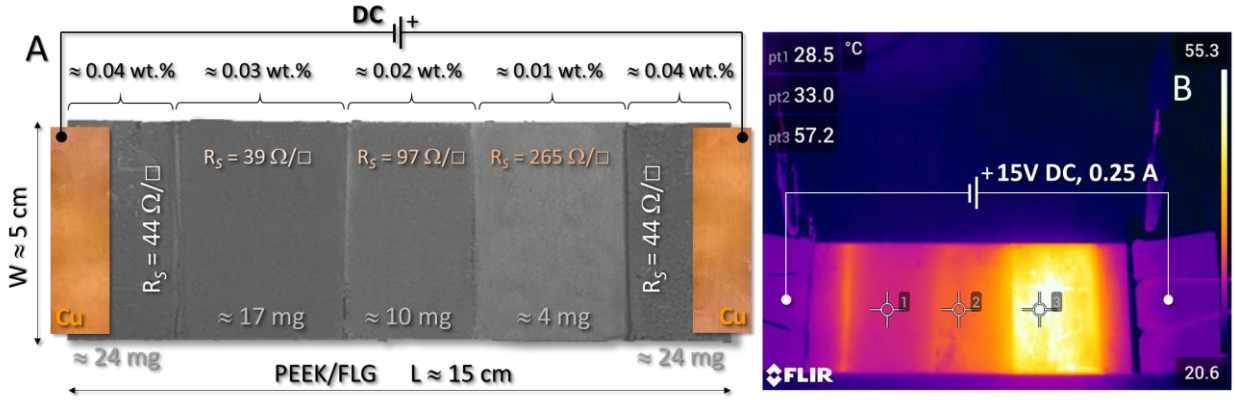

Fig. 8. A) A PEEK plate covered with thin FLG coatings obtained by airbrush painting selected portion of the plate with different graphene loadings. Each portion was painted using a 3g/L suspension of FLG sheets. 10, 8, 4, 1.5 and 10 mL of the suspension were used to coat the plate portions from left to right, respectively. B) Infrared thermal map of the composite surface temperature once an external 15V power supply was applied. pt1-pt3 refer to the plate temperature values on three plate positions featured by an increasing surface resistance.

The electro-thermal de-icing properties of the conductive polymer-based composites prepared using the airbrush-painting/drying protocol have been finally tested on a model ABS 3D printed A-10 airplane reproduced on a 1:133 scale with a final weight of 12.51 g and a calculated surface area of ≈ 78.4 cm^2 (Fig. S12A). As briefly discussed earlier, the search for new, effective and scalable de-icing solutions based on the development of conductive and lightweight composites is gaining particular interests from the aerospace and the civil engineering field. This is particularly relevant when lightweight materials suitable to operate under unconventional cold climate conditions are

required. The ABS airplane model underwent two successive airbrush-paining/drying cycles using a 5 mL of a 3 g/L aqueous suspension of FLG sheets for each painting/coating cycle. As a result, a ≈ 0.2 wt.% FLG/ABS composite was prepared (≈ 0.3 mg/cm^2 of FLG; overall ≈ 24 mg of FLG). Its surface resistance was directly measured on a portion of the model using the four-terminal sensing probe and it was fixed to 101 Ω/□.

In a first heating trial, the ABS model was exposed to liquid N_2 vapors and cooled down to -40 °C before connecting its wings ends to an external DC power supply of 24 V and closing the electrical circuit. The aircraft surface temperature was monitored with the FLIR thermal camera just after removing the liquid nitrogen and closing the circuit. The full sequence of the infrared thermal mapping is shown in Fig. S12 and it unveils the rapid and homogeneous heating of the surface comprises between the two electrical clamps. Starting from -40 °C, the wings temperature grew-up close to ≈ +14, ≈ +42, ≈ +78 °C after 60, 120 and 180 seconds. In a further attempt to demonstrate the deicing properties of the composite under more realistic conditions, the aircraft model was left at -18 °C for 12 hours during which its surface was periodically irrorated with water as to force the generation of ice deposits on its whole surface and on the wings mainly. Afterwards, the application of the external DC 24 V power supply led to the progressive deicing of the model within few minutes. Fig. 9 shows the stepwise deicing procedure since T = 0 s (Fig. 9A) up to 360 s of closed circuit, during which ice was completely melt and the composite temperature reached up to ≈ 130 °C (Fig. 9B-E, 9C-F and 9D-G). As shown by digital photos in Fig. 9, one aircraft wing was preliminarily covered with a protective white acrylic paint. Noteworthy, the ice melting rate observed on the latter was even faster than that occurring on the unprotected one. Such an effect was ascribed to a reduced dissipation of the heat produced by the underneath graphene coating because of a “heat confinement” effect fostered by to the protective action of the outmost painted layer.

The electro-thermal action of the FLG coating can also be regarded as a low-energy consuming system for preventing the surface ice generation. Indeed, a constantly applied low voltage can be sufficient to generate a thin water layer on the surface of a selected device (melting only a thin layer of interfacial ice) hence causing the ice slide off on the resulting thin water film.[25]

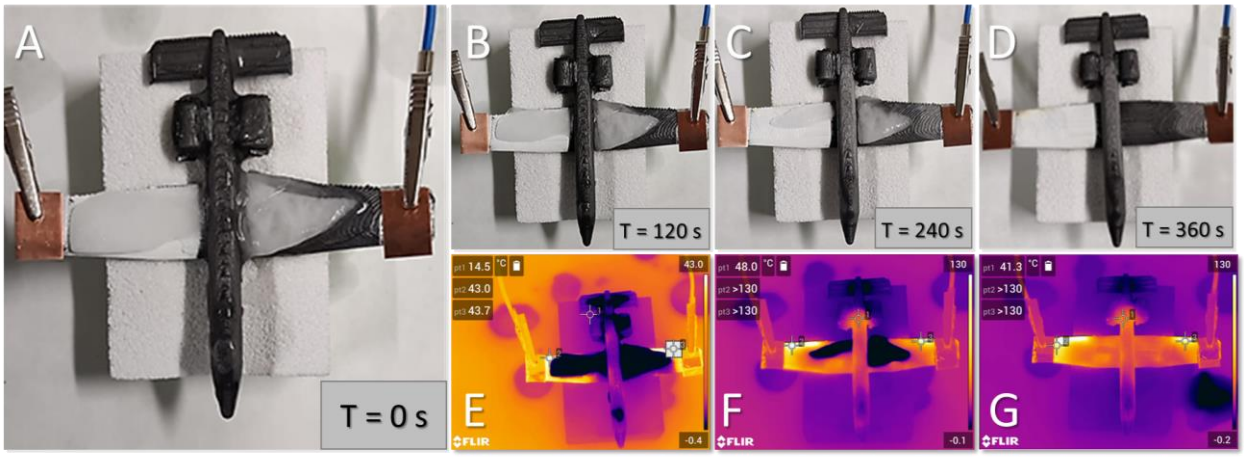

Fig. 9. A) Digital photo of a ≈ 0.2 wt.% ABS/FLG aircraft model at T = 0 s, after the forced ice generation on its surface/wings. B-G) Digital photos (B-D) and infrared surface thermal images (E-G) recorded after the application of an external DC power supply of 24 V and acquired at regular time intervals of 120 (B-E), 240 (C-F) and 360 (D-G) seconds, respectively. pt1-pt3 refer to the aircraft surface temperature values on three different positions.

Conclusions

Most polymers possess low electrical conductivity or more often are electrical insulators and thus their application as electrothermal materials is deeply limited if not completely inhibited. This contribution described a convenient and easily scalable approach to the preparation of conductive polymer-based composites using a stable FLG-based overcoat prepared at the outmost polymer surface. The FLG/polymer interface adhesion is strengthened through a controlled thermal post-treatment of the composite to a temperature close to that of its glass transition. Accordingly, the elastic and viscoelastic response of the amorphous and semi-crystalline phases of the polymer facilitate the homogeneous adhesion of the thin FLG deposit while maintaining the bulk polymer properties almost unchanged. The excellent FLG adhesion along with the formation of percolative electric networks already for very small amounts of FLG charges, hold important benefits on the

electrothermal properties of the as-prepared composites as well as on their ultimate lightweight character. These features along with the straightforward, cheap, and easily scalable production method, make the composites from this series highly attractive materials for targeted application, particularly in dedicated sectors of aerospace and civil engineering. Indeed, lightweight components or devices with a low-power control of their surface temperature or de-icing properties can find concrete applications in several technological daily-life fields.

We have presented several examples of how our technology can set the way to various real-world applications: from the preparation of planar composite radiators with 0.1 wt.% of FLG as low-power, indoor heating devices to thermo-stabilized piping for the transport of thermo-sensitive fluids up to a next generation composites with stable and low-power heatable overcoats for the cheap and eco-friendly de-icing.

Conflict of interest

The authors declare no conflict of interest.

Acknowledgements

The authors would like to thank the SATT-Conectus for financial support through the GRAPHIC project. G. G. and C. P.-H. would also like to thank the TRAINER project (Catalysts for Transition to Renewable Energy Future) of the "Make our Planet Great Again" program (Ref. ANR-17-MPGA-0017) for support. G.G. would also like to thank the Italian MIUR through the PRIN 2017 Project Multi-e (20179337R7) "Multielectron transfer for the conversion of small molecules: an enabling technology for the chemical use of renewable energy" for financial support to this work. The SEM and XPS experiments were carried out at the SEM and XPS platforms of the ICPEES-IPCMS units and Dr. V. Papaefthimiou (ICPEES) is gratefully acknowledged for performing XPS analysis. TEM experiments were carried out at the TEM platform of the IPCMS and Dr. W. Baaziz and Prof. O. Ersen are gratefully acknowledged.

References and Notes

[1] M.H. Naveen, N.G. Gurudatt, Y.-B. Shim, Applications of conducting polymer composites to electrochemical sensors: A review, App. Mater. Today 9 (2017) 419-433.

[2] J. Yang, Y. Liu, S. Liu, L. Li, C. Zhang, T. Liu, Conducting polymer composites: material synthesis and applications in electrochemical capacitive energy storage, Mater. Chem. Front. 1 (2017) 251-268.

[3] A. Li, C. Zhang, Y.F. Zhang, Thermal Conductivity of Graphene-Polymer Composites: Mechanisms, Properties, and Applications, Polymers 9 (2017) 437 (17).

[4] T. Kuilla, S. Bhadra, D. Yao, N.H. Kim, S. Bose, J.H. Lee, Recent advances in graphene based polymer composites, Prog. Polymer Sci. 35 (2010) 1350-1375.

[5] Y. Lu, Y. Song, F. Wang, Thermoelectric properties of graphene nanosheets-modified polyaniline hybrid nanocomposites by an in situ chemical polymerization, Mater. Chem. Phys. 138 (2013) 238-244.

[6] A.-R.O. Raji, T. Varadhachary, K. Nan, T. Wang, J. Lin, Y. Ji, B. Genorio, Y. Zhu, C. Kittrell, J.M. Tour, Composites of Graphene Nanoribbon Stacks and Epoxy for Joule Heating and Deicing of Surfaces, ACS Appl. Mater. Interf. 8 (2016) 3551-3556.

[7] T. Wang, Y. Zheng, A.-R.O. Raji, Y. Li, W.K.A. Sikkema, J.M. Tour, Passive Anti-Icing and Active Deicing Films, ACS Appl. Mater. Interf. 8 (2016) 14169-14173.

[8] N. Karim, M. Zhang, S. Afroj, V. Koncherry, P. Potluri, K.S. Novoselov, Graphene-based surface heater for de-icing applications, RSC Adv. 8 (2018) 16815-16823.

[9] D. Amoabeng, S.S. Velankar, A Review of Conductive Polymer Composites Filled With Low Melting Point Metal Alloys, Polymer Eng. Sci. 58 (2018) 1010-1019.

[10] A.R. Ajitha, T. Sabu, Compatibilization of Polymer Blends, in: A.R. Ajitha, T. Sabu (Eds.), Compatibilization of Polymer Blends, Elsevier2019, p. 640.

[11] E.A. Coleman, Plastics Additives, in: M. Kutz (Ed.), Applied Plastics Engineering Handbook - Processing and Materials, Elsevier Inc.2011, pp. 419-428.

[12] M. Šupová, G.S. Martynková, K. Barabaszová, Effect of Nanofillers Dispersion in Polymer Matrices: A Review, Sci. Adv. Mater. 3 (2011) 1-25.

[13] Y. Guo, X. Zuo, Y. Xue, J. Tang, M. Gouzman, Y. Fang, Y. Zhou, L. Wang, Y. Yu, M.H. Rafailovich, Engineering thermally and electrically conductive biodegradable polymer nanocomposites, Composites Part B 189 (2020) 107905.

[14] X. He, Y. Wang, Recent Advances in the Rational Design of Thermal Conductive Polymer Composites, Ind. Eng. Chem. Res. 60 (2021) 1137-1154.

[15] H. Zhang, X. Zhang, Z. Fang, Y. Huang, H. Xu, Y. Liu, D. Wu, J. Zhuang, J. Sun, Recent Advances in Preparation, Mechanisms, and Applications of Thermally Conductive Polymer Composites: A Review, J. Compos. Sci. 4 (2020) 180.

[16] O. Fakorede, Z. Feger, H. Ibrahim, A. Ilinca, J. Perron, C. Masson, Ice Protection Systems for Wind Turbines in Cold Climate: Characteristics, Comparisons and Analysis, Renewable Sustainable Energy Rev. 65 (2016) 662-675.

[17] J. Palacios, E. Smith, J. Rose, R. Royer, Ultrasonic De-Icing of Wind-Tunnel Impact Icing, J. Aircr. 48 (2011) 1020-1027.

[18] L. Vertuccio, F. De Santis, R. Pantani, K. Lafdi, L. Guadagno, Effective de-icing skin using graphene-based flexible heater, Composites Part B 162 (2019) 600-610.

[19] B.G. Falzon, P. Robinson, S. Frenz, B. Gilbert, Development and evaluation of a novel integrated anti-icing/de-icing technology for carbon fibre composite aerostructures using an electro-conductive textile, Composites Part B 68 (2015) 323-335.

[20] X. Yao, S.C. Hawkins, B.G. Falzon, An advanced anti-icing/de-icing system utilizing high aligned carbon nanotubes webs, Carbon 136 (2018) 130-138.

[21] Record of Conference Papers Industry Applications Society 52nd Annual Petroleum. A. Nysveen, H. Kulbotten, Lervik, A.H. Bomes, M. Høyer-Hansen, Direct electrical heating of subsea pipelines - technology development and operating experience, (2005) 177-187.

[22] HighPEEK - Conductive Plastics for Satellite Parts - European Space Agency (ESA) (https://artes.esa.int/projects/highpeek) (last access April 15, 2021).

[23] W.O. Valarezo, F.T. Lynch, R.J. McGehee, Aerodynamic Performance Effects due to Small Leading-Edge Ice (Roughness) on Wings and Tails, J. Aircr. 30 (1993) 807-812.

[24] F.T. Lynch, A. Khodadoust, Effects of Ice Accretions on Aircraft Aerodynamics, Prog. Aerosp. Sci. 37 (2001) 669-767.

[25] V.F. Petrenko, C.R. Sullivan, V. Kozlyuk, F.V. Petrenko, V. Veerasamy, Pulse electro-thermal de-icer (PETD), Cold Reg. Sci. Technol. 65 (2011) 70-78.

[26] D.M. Ramakrishna, T. Viraraghavan, Environmental impact of chemical de-icers - A review, Water Air Soil Pollut. 166(49-63) (2005) 49.

[27] P.G. Karagiannidis, S.A. Hodge, L. Lombardi, F. Tomanchio, N. Decorde, S. Milana, I. Goykhman, Y. Su, S.V. Mesite, D.N. Johnstone, R.K. Leary, P.A. Midgley, N.M. Pugno, F. Torrisi, A.C. Ferrari, Microfluidization of Graphite and Formulation of Graphene-Based Conductive Inks, ACS Nano 11 (2017) 2742-2755.

[28] H. Ba, L. Truong-Phuoc, V. Papaefthimiou, C. Sutter, S. Pronkin, A. Bahouka, Y. Lafue, L. Nguyen-Dinh, G. Giambastiani, C. Pham-Huu, Cotton Fabric Coated with Few-Layer Graphene as Highly Responsive Surface Heaters and Integrated Lightweight E-Textiles Circuits, ACS Appl. Nano Mater. 3 (2020) 9771-9783.

[29] Y. Zhu, S. Murali, M.D. Stoller, K. Ganesh, W. Cai, P.J. Ferreira, A. Pirkle, R.M. Wallace, K.A. Cychosz, M. Thommes, Carbon-Based Supercapacitors Produced by Activation of Graphene, Science 332 (2011) 1537-1541.

[30] H. Chen, M.B. Muller, K.J. Gilmore, G.G. Wallace, D. Li, Mechanically Strong, Electrically Conductive, and Biocompatible Graphene Paper, Adv. Mater. 20 (2008) 3557-3561.

[31] A.K. Geim, Graphene: Status and Prospects, Science 324 (2009) 1530-1534.

[32] E. Pop, D. Mann, Q. Wang, K. Goodson, H. Dai, Thermal Conductance of An Individual Single-Wall Carbon Nanotube Above Room Temperature, Nano Lett. 6 (2006) 96-100.

[33] Y. Arao, Y. Mizuno, K. Araki, M. Kubouchi, Mass Production of High-Aspect-Ratio Few-Layer-Graphene by High-Speed Laminar Flow, Carbon 102 (2016) 330-338.

[34] H. Ba, C. Sutter, A. Bahouka, Y. Lafue, L. Nguyen-Dinh, C. Pham-Huu Méthode de fabrication d'un composite conducteur comprenant au moins une couche superficielle comprenant du graphène multi-feuillets. French Pat. Appl. No. 18-59684, CNRS, University of Strasbourg and BlackLeaf SAS, 2018.

[35] C. Pham-Huu, H. Ba, A. Bahouka, Y. Lafue Procédé de réalisation, d'application et de fixation d'un revêtement de surface multicouches à base de matériau(x) 2D et/ou carboné(s) sur un substrat hôte et dispositif de substrat hôte susceptible d'être obtenu par ledit procédé. French Pat. Appl. No. FR 18-71908, BlackLeaf SAS, CNRS and University of Strasbourg, 2018.

[36] H. Ba, C. Sutter, V. Papaefthimiou, S. Zafeiratos, A. Bahouka, Y. Lafue, L. Nguyen-Dinh, T. Romero, C. Pham-Huu, Foldable flexible electronics based on few-layer graphene coated onpaper composites, Carbon 167 (2020) 169-180.

[37] R_S is commonly defined as the resistivity (ρ) of a given material divided by its thickness (t): $R_S = \rho/t$ expressed as Ω/□.

[38] X. Gao, N. Yokota, H. Oda, S. Tanaka, K. Hokamoto, P. Chen, M. Xu, Preparation of Few-Layer Graphene by Pulsed Discharge in Graphite Micro-Flake Suspension, Crystals 9 (2019) 150 (13).

[39] A.C. Ferrari, J.C. Meyer, V. Scardaci, C. Casiraghi, M. Lazzeri, F. Mauri, S. Piscanec, D. Jiang, K.S. Novoselov, S. Roth, A.K. Geim, Raman Spectrum of Graphene and Graphene Layers, Phys. Chem. Lett. 97 (2006) 187401 (4).

[40] F. Farivar, P.L. Yap, K. Hassan, T.T. Tung, D.N.H. Tran, A.J. Pollard, D. Losic, Unlocking thermogravimetric analysis (TGA) in the fight against “Fake graphene” materials, Carbon 179 (2021) 505-513.

[41] International Organization for Standardization (ISO), in Nanotechnologies – Vocabulary – Part 13: Graphene and Related Two-Dimensional (2D) Materials, BSI Standards Publication, London, UK 2017.

[42] P. Bøggild, The war on fake graphene, Nature 562 (2018) 502-503.

[43] A.P. Kauling, A.T. Seefeldt, D.P. Pisoni, R.C. Pradeep, R. Bzentini, R.V.B. Oliveira, K.S. Novoselov, A.H. Castro Neto, The Worldwide Graphene Flake Production, Adv. Mater. (2018) 1803784 (6).

[44] C. Mattevi, G. Eda, S. Agnoli, S. Miller, K.A. Mkhoyan, O. Celik, D. Mastrogiovanni, G. Granozzi, E. Garfunkel, M. Chhowalla, Evolution of Electrical, Chemical, and Structural Properties of Transparent and Conducting Chemically Derived Graphene Thin Films, Adv. Funct. Mater. 19 (2009) 2577-2583.

[45] D.X. Yang, A. Velamakanni, G. Bozuklu, S. Park, M. Stoller, R.D. Piner, S. Stankovich, I. Jung, D.A. Field, C.A. Ventrice Jr, R.S. Ruoff, Chemical Analysis of Graphene Oxide Films after Heat and Chemical Treatments by X-Ray Photoelectron, Carbon 47 (2009) 145-152.

[46] J.I. Paredes, S. Villar-Rodil, A. Martinez-Alonso, J.M.D. Tascon, Graphene Oxide Dispersions in Organic Solvents, Langmuir 24 (2008) 10560-10564.

[47] S. Gayathri, P. Jayabal, M. Kottaisamy, V. Ramakrishnan, Synthesis of few layer graphene by direct exfoliation of graphite and a Raman spectroscopic study, AIP Advances 4 (2014) 027116 (12).

[48] The image was acquired with a tilted angle of nearly +10° respect to the basal plain of the composite; therefore the estimated thickness of the FLG deposit was expressed as follows: 4/cos(10) = 4.06 μm that falls in the range of tickness for the FLG deposit (± 1 μm).

[49] N. Karim, S. Afroj, S. Tan, P. He, A. Fernando, C. Carr, K.S. Novoselov, Scalable Production of Graphene-Based Wearable E-Textiles, ACS Nano 11 (2017) 12266-12275.

[50] R. Ramasubramaniam, J. Chen, H. Liu, Homogeneous carbon nanotube/polymer composites for electrical applications, Appl. Phys. Lett. 83 (2003) 2928-2930.

[51] For a random distribution of CNT as electrically conductive fillers, a conducting network will form at a specific filler loading, known as the percolation threshold (pc). When the filler loading reaches pc, the conductivity of the composite rises suddenly and the graph of conductivity versus loading takes the characteristic S-shape, demonstrating the three characteristic regimes of the composite: insulating, percolating and conductive. See ref. 53.

[52] W. Bauhofer, J.F. Kovacs, A review and analysis of electrical percolation in carbon nanotube polymer composites, Compos. Sci. Technol. 69 (2009) 1486-1498.

[53] A.J. Marsden, D.G. Papageorgiou, C. Vallés, A. Liscio, V. Palermo, M.A. Bissett, R.J. Young, I.A. Kinloch, Electrical percolation in graphene–polymer composites, 2D Mater. 5 (2018) 032003 (19).

[54] P.S. Anbinder, P.J. Peruzzo, A. de Siervo, J.I. Amalvy, Surface, thermal, and mechanical properties of composites and nanocomposites of polyurethane/PTFE nanoparticles, J. Nanopart. Res. 16 (2014) 2529 (11).

[55] W. Wang, G. Tuci, C. Duong-Viet, Y. Liu, A. Rossin, L. Luconi, J.-M. Nhut, L. Nguyen-Dinh, C. Pham-Huu, G. Giambastiani, Induction Heating: an Enabling Technology for the Heat Management in Catalytic Processes, ACS Catal. 9 (2019) 7921-7935.

[56] C. Appino, O. De La Barrière, F. Fiorillo, M. Lobue, F. Mazaleyrat, C. Ragusa, Classical eddy current losses in Soft Magnetic Composites, J. Appl. Phys. 113 (2013) 17A322 (3).

[57] J. Corcoran, P.B. Nagy, Compensation of the Skin Effect in Low-Frequency Potential Drop Measurements, J. Nondestruct. Eval. 35 (2016) 58.

[58] A. Skumiel, M. Kaczmarek-Klinowska, M. Timko, M. Molcan, M. Rajnak, Evaluation of Power Heat Losses in Multidomain Iron Particles Under the Influence of AC Magnetic Field in RF Range, Int. J. Thermophys. 34 (2013) 655-666.

Graphical Abstract

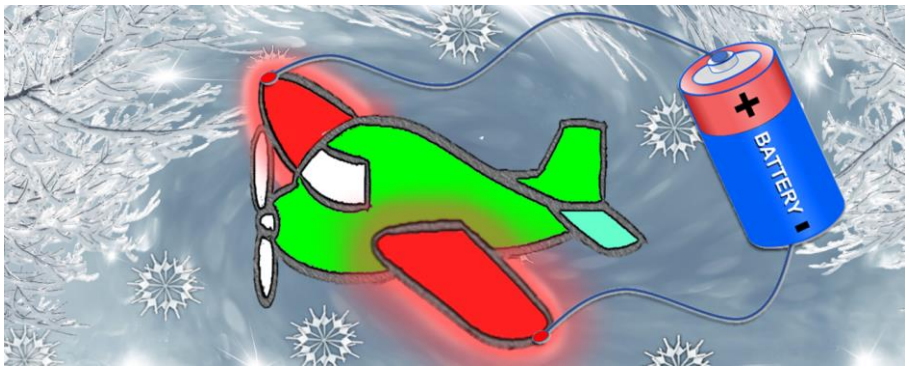

Figure(s)

Click here to access/download;Figure(s);Fig. 1.tif

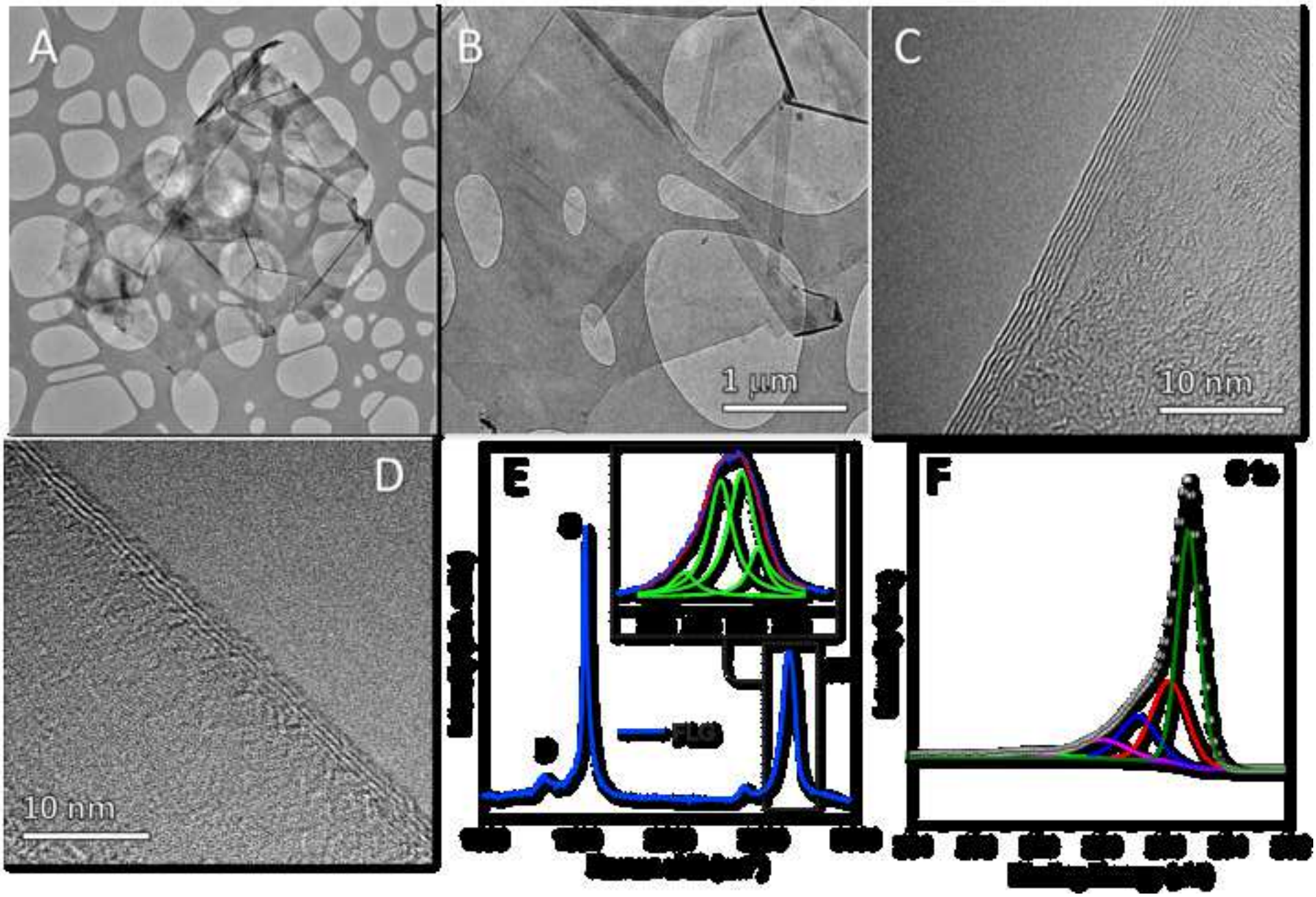

Figure(s)

Click here to access/download;Figure(s);Fig. 2.tif

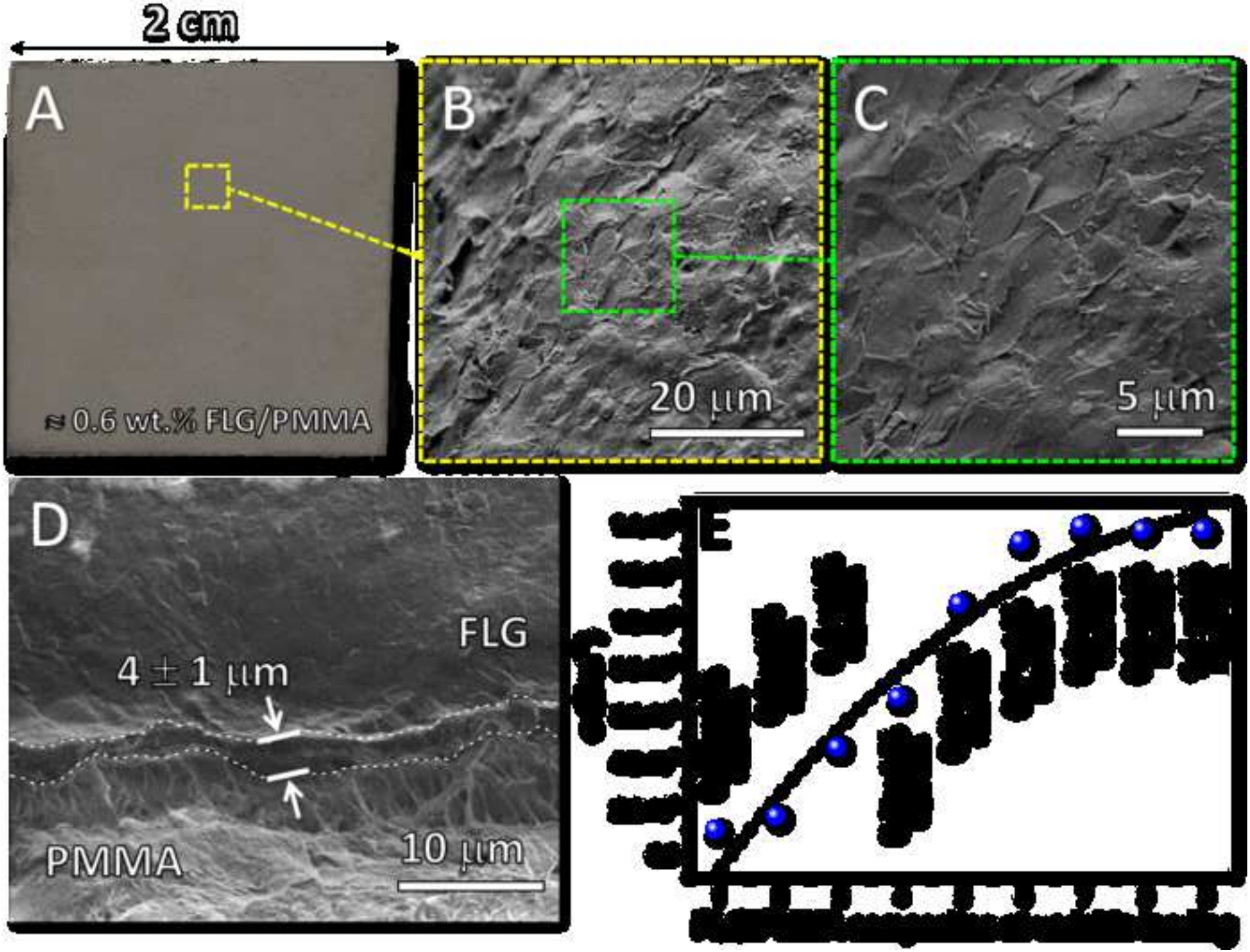

Figure(s)

Click here to access/download;Figure(s);Fig. 3.tif

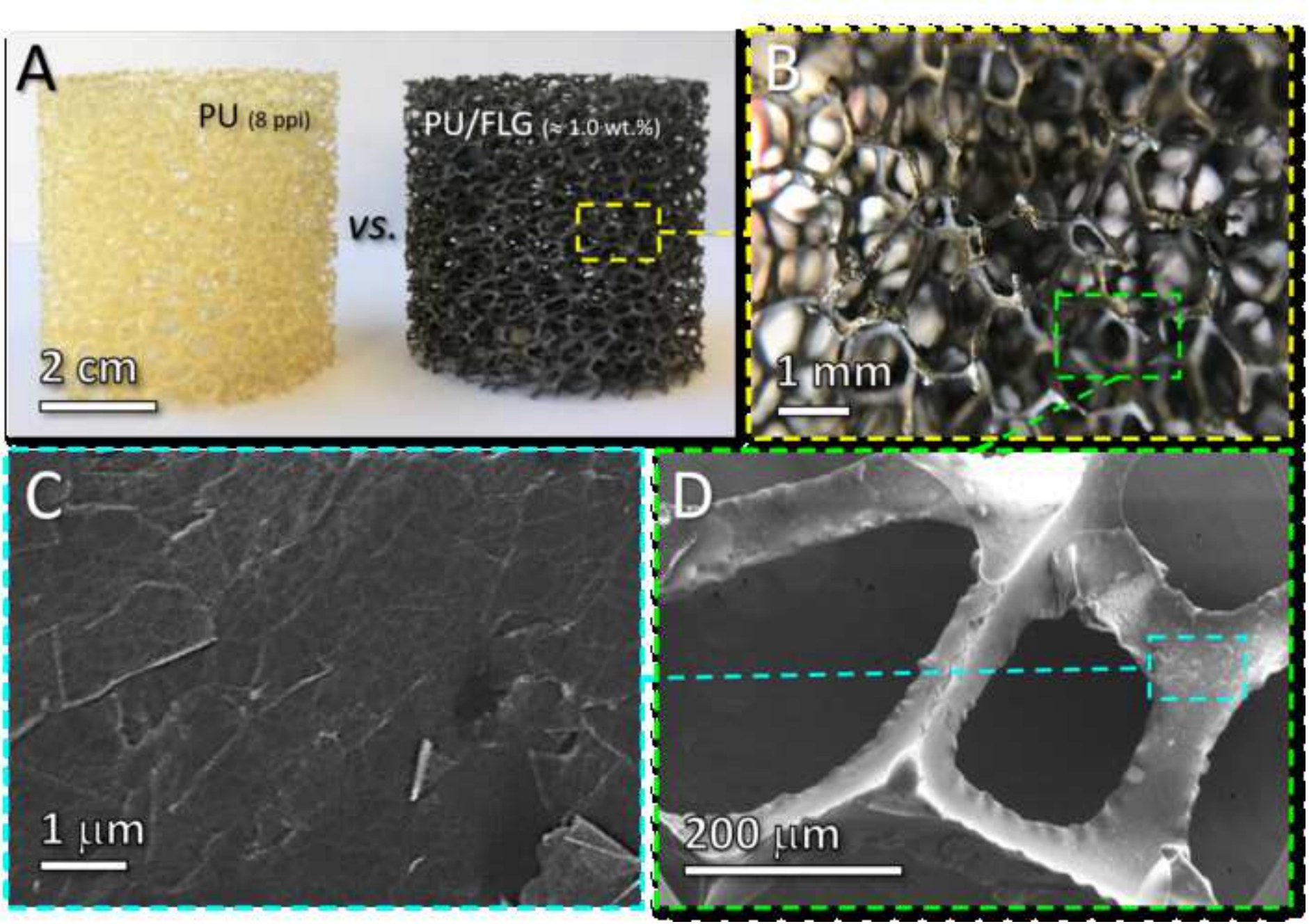

Figure(s)

Click here to access/download;Figure(s);Fig. 4.tif

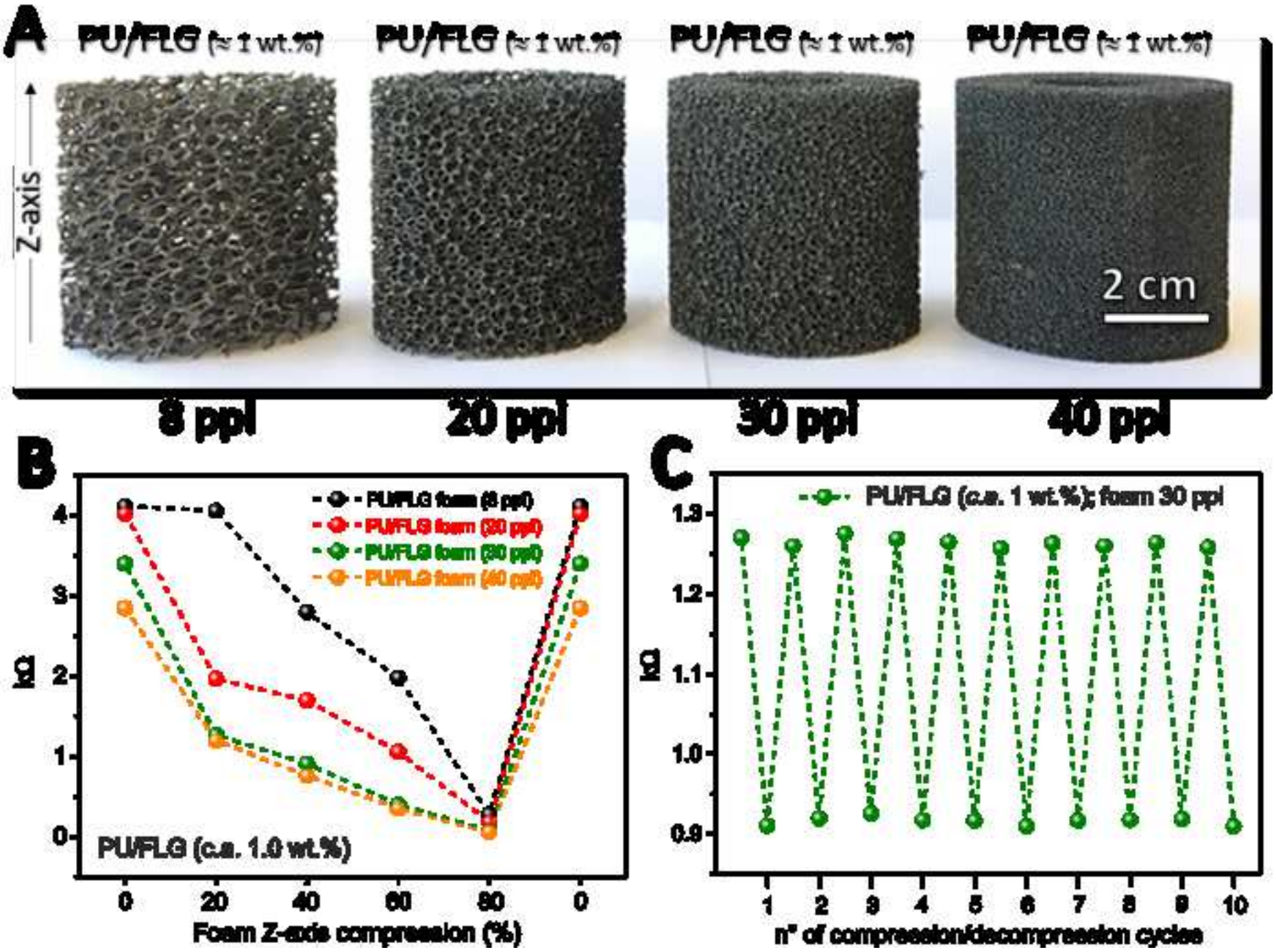

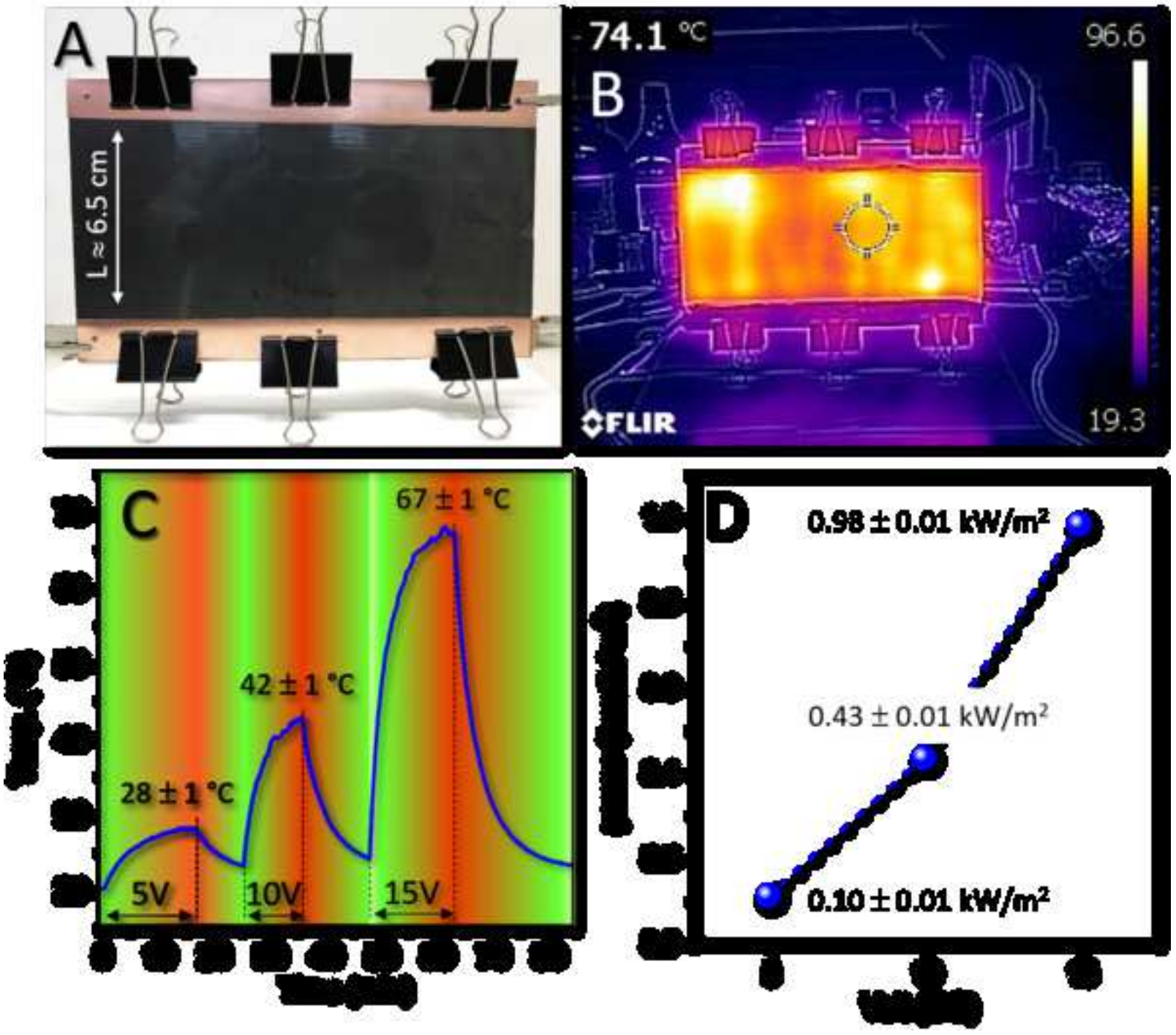

Figure(s)

Click here to access/download;Figure(s);Fig. 6.tif

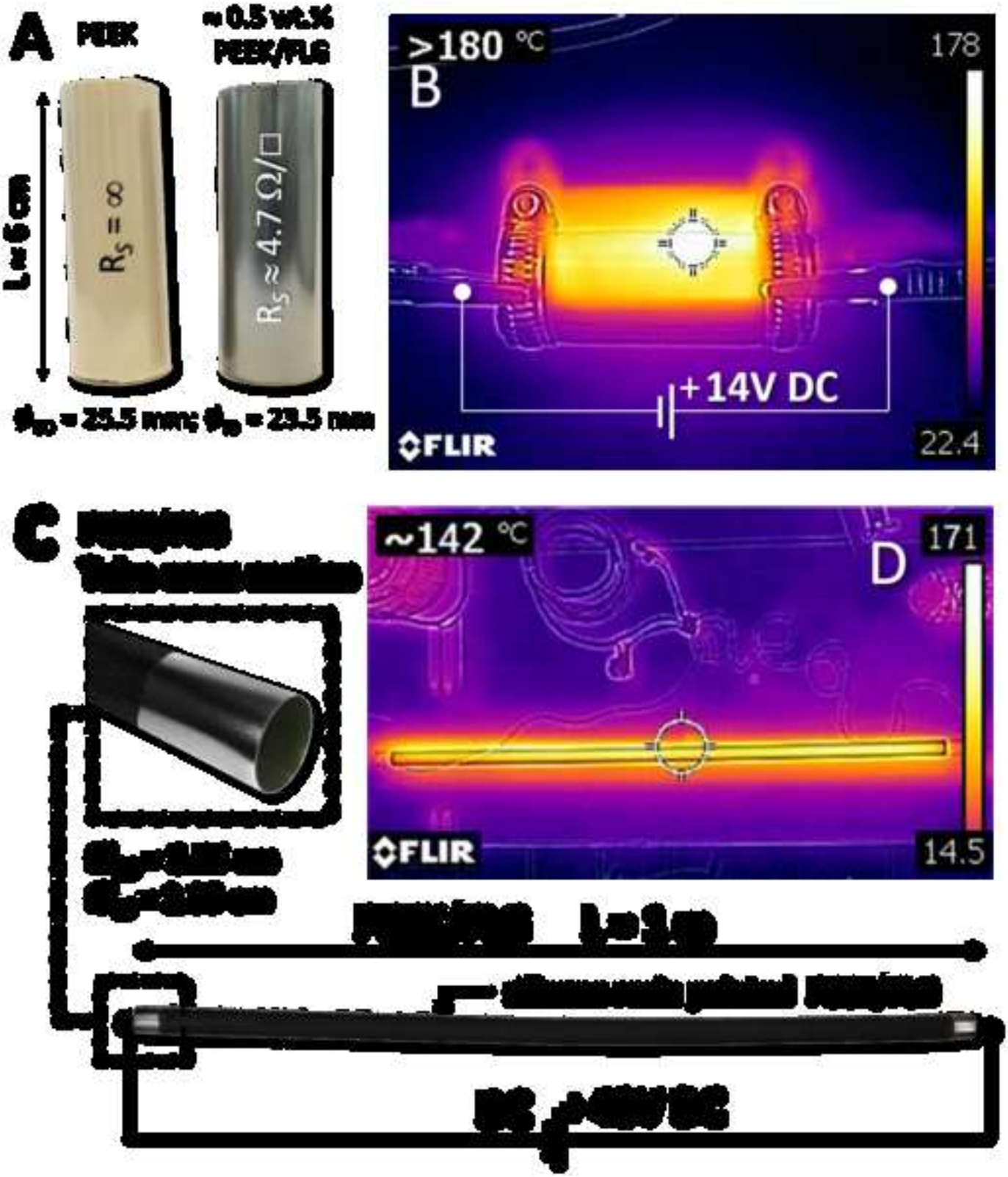

Figure(s)

Click here to access/download;Figure(s);Fig. 7.tif

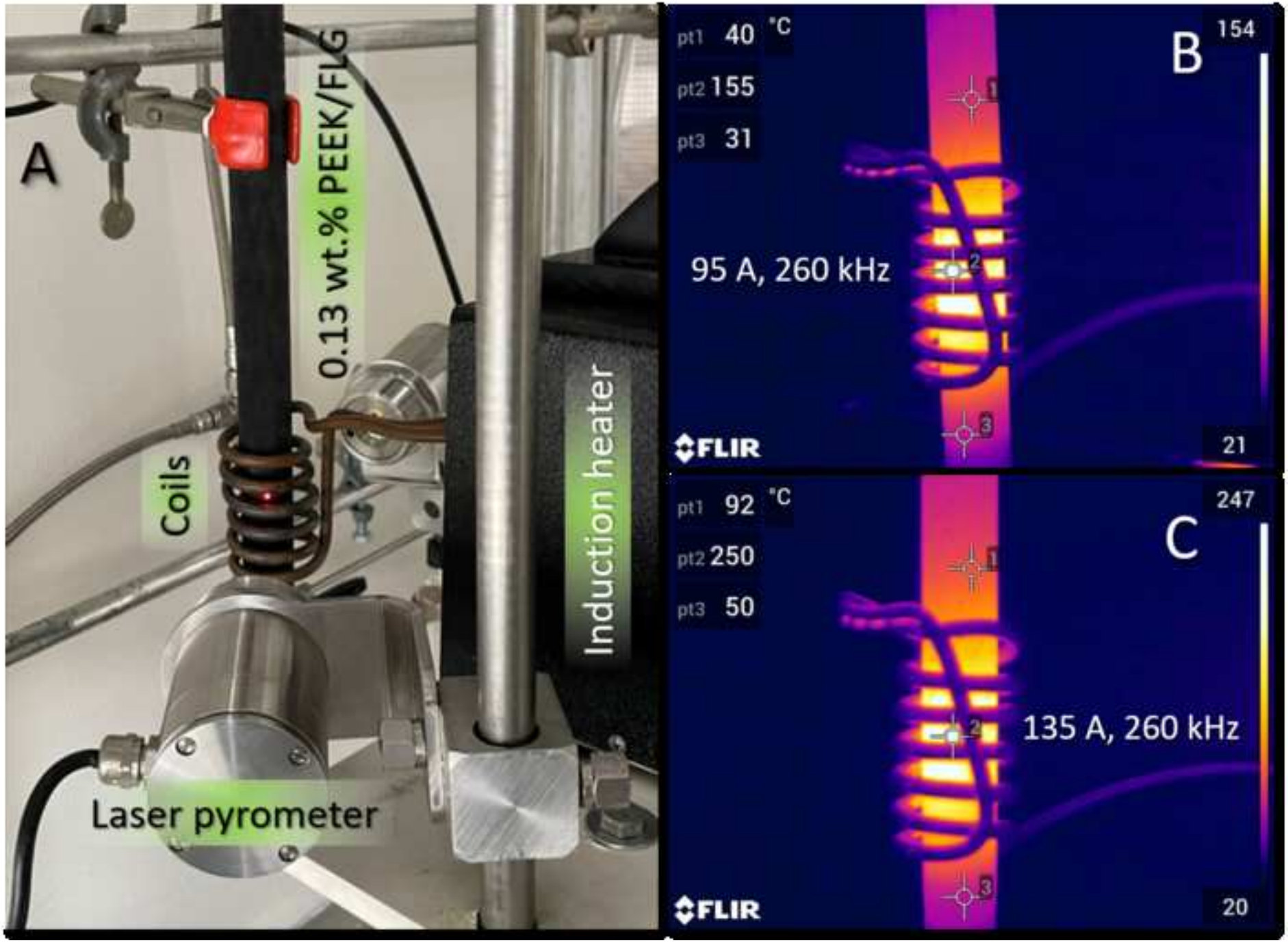

Figure(s)

Click here to access/download;Figure(s);Fig. 8.tif

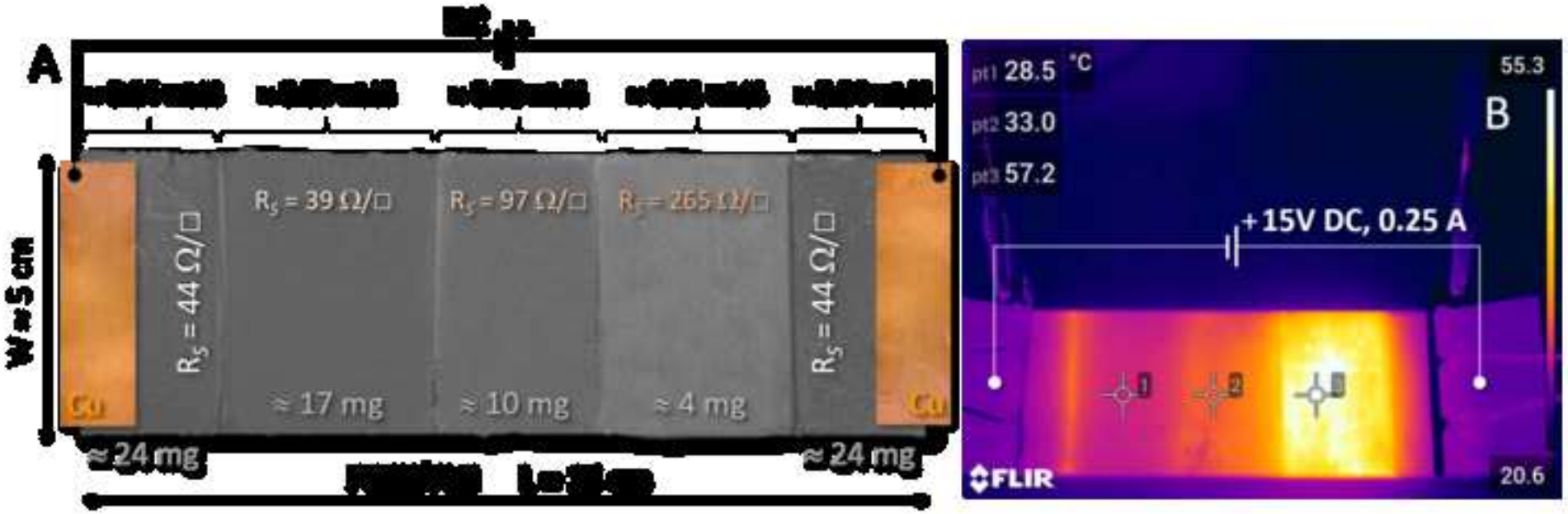

Figure(s)

Click here to access/download;Figure(s);Fig. 9.tif